MAPPING PEAT DEPTH AND SMOULDERING VULNERABILITY

MAPPING PEAT DEPTH USING REMOTE SENSING AND MACHINE LEARNING TO IMPROVE PEAT SMOULDERING VULNERABILITY PREDICTION

By EMMA SHERWOOD, B. Sc.

A Thesis Submitted to the School of Graduate Studies in Partial Fulfillment of the Requirements for the Degree of Master of Science

McMaster University MASTER OF SCIENCE (2023)

Hamilton, Ontario, Canada (School of Earth, Environment & Society)

TITLE: Mapping Peat Depth Using Remote Sensing and Machine Learning to Improve Peat Smouldering Vulnerability Prediction

AUTHOR: Emma Sherwood, B.Sc. (University of British Columbia)

SUPERVISOR: Dr. James M. Waddington

NUMBER OF PAGES: xiii, 85

Lay Abstract

Peat is organic soil made from decomposing plant material. Peat can burn, especially in the hot, dry weather which is happening more often due to climate change. Dense, dry peat is more vulnerable to fire: it will burn more deeply. Because it is known that areas with deeper peat can retain moisture better, peat depth can be used as a proxy for vulnerability to fire. Since peat depth is expensive and time consuming to map directly, remotely sensed data such as aerial imagery was used in a model to predict peat depths. The model was able to predict peat depths and displayed that the most vulnerable areas are scattered across the landscape in small patches. This project also found that denser peat is found farther from the surface in deeper peat areas, further supporting the use of peat depth as a proxy for vulnerability to smouldering.

Abstract

Peat is an accumulation of soil formed from partially decomposed organic matter. Peat can burn, especially in hot, dry weather which is happening more often due to climate change; smouldering releases stored carbon to the atmosphere. Peat that has higher organic bulk density and lower moisture content is more vulnerable to fire: it will burn more severely (more deeply) if ignited. Shallower peat is less able to retain moisture during droughts and is therefore likely more vulnerable to fire; however, mapping peat depths at high spatial resolution is expensive or requires extensive fieldwork. This project uses remote sensing in combination with machine learning to estimate peat depth across a peatland and rock barren landscape. A Random Forest model was used to map peat depths across the landscape at a 1 m spatial resolution using LiDAR data and orthophotography. The resulting map was able to predict peat depths (R^2 = 0.73, MAE = 28 cm) and showed that the peat depths which are especially vulnerable to high severity fire are distributed in numerous small patches across the landscape. This project also examined peat bulk density and found that the Von Post scale for peat decomposition can be used as a field method for estimating bulk density (R^2 = 0.71). In addition, in this landscape, peat bulk densities at the same depth (within the top 45 cm) are higher in shallower peat because in shallower peat, more decomposed peat was found closer to the surface, and because peat with high mineral content was found close to the bedrock or mineral soil. The findings of this project will be valuable for wildfire managers to determine which areas on the

landscape are most vulnerable to fire, allowing them to mobilize resources more rapidly for wildfire suppression.

Acknowledgements

There are so many people who I need to thank for their support on my journey through writing this thesis. Firstly, my supervisor Mike Waddington, who has been incredibly patient, positive, and supportive throughout the duration of my degree, and crucial in helping me overcome challenges I've faced. Guidance and assistance from Sophie, Chantel, Paul, and Colin has been indispensable. Alex F, Greg, Alex T, Gracie, Justin, Hope and Renée have all been great field partners and lab mates. Thank you for brainstorming and problem solving in the field, making me feel like part of the team, teaching me how to be a master's student, joining me for post-fieldwork climbing and, of course, helping me with the fieldwork itself. Thank you to the McMaster Ecohydrology lab in general!

Thanks Mom, Dad, and the rest of my relatives in Alberta for not letting the distance and the pandemic prevent me from feeling like part of the family. Thank you to Isaac for always being ready to cheer me on when I needed more motivation and being willing to listen to me complain about whatever struggle I was facing.

Thank you to all the 22 people and two dogs I shared a house with at some point throughout my degree, especially the many heartfelt chats, shared meals, laughs and good times. Bonus shoutout for Emma W. for also helping me out with a couple days of fieldwork. To Pia and Erin, thank you for your phone calls that kept me sane and connected throughout the pandemic. Thank you to my wonderful quadball friends and teammates (on and off the pitch); many great road trips, practices and games were a key break from thesis writing.

Finally, to my past and present mentors and coworkers in GIS and field jobs from Prince George, Saskatoon, Medicine Hat and Waterloo, and many teachers and professors throughout my academic journey – thank you for all the learning and encouragement, without which I never would have gotten here.

Table of Contents

List of Figures

List of Abbreviations

COOP: Central Ontario Orthophotography Product

DEM: Digital Elevation Model

DSM: Digital Surface Model

GIS: Geographic Information Sciences/Systems

LiDAR: Light Detection and Ranging

LOI: Loss On Ignition

MBD: Mineral bulk density

NDVI: Normalized Differential Vegetation Index

NDWI: Normalized Differential Water Index

NIR: Near Infrared band

OBD: Organic bulk density

PS33: Parry Sound 33 wildfire

RF: Random Forest

TWI: Topographic Wetness Index

- MD8: Multidirectional flow
- MDInf: Triangular multiple flow direction
- SWI: SAGA Wetness Index

TPI: Topographic Position Index

VP: Von Post

Declaration of Academic Achievement

This thesis contains written material prepared solely by this author. Chapters one and four provide a general introduction and conclusion, respectively. Chapters two and three are data chapters intended for future peer review and publishing.

Dr. Mike Waddington was key in developing the research design; additional input on research design was received from Dr. Chantel Markle and Dr. Sophie Wilkinson. Dr. Chantel Markle was also instrumental in the application of the linear mixed effects model. Dr. Sophie Wilkinson assisted in determining protocols for lab work. Alex Furukawa, Alex Tekatch, Emma Waddington, Gracie Crafts, Greg Verkaik, Justin Kruse, and Mike Waddington assisted with fieldwork: peat depth measurements, taking peat samples, and recording additional data.

Chapter 1: Introduction

Background

Peat is an accumulation of soil formed from partially decomposed organic matter. Across Canada, 12% of the country is covered by peatlands, storing 56% of the country's soil organic carbon (Tarnocai, 2006). Peat can smoulder: it combusts slowly without flames, meaning the oxidation reaction is occurring at the surface or within the peat matrix, rather than in nearby gas, as is the case in flaming (Ohlemiller, 1985; Rein, 2009). When peat smoulders, it emits CO_2 to the atmosphere through the combustion of legacy carbon that has long been stored in the peat (Turetsky et al., 2002; Wilkinson et al., 2018). In addition, peat smouldering damages soil (Kettridge et al., 2014) emits pollutants (Rein, 2009), harms human health (Liu et al., 2015), and more recently has been shown to impact species at risk habitat (e.g. Markle et al., 2020). Because climate change and anthropogenic disturbances are leading to more severe, frequent and extensive peat fires (Turetsky et al., 2014; Wilkinson et al., 2023), there is a need to better understand and map peat vulnerability to fire to enable better peatland and wildfire management to mitigate these impacts.

Peat properties and smouldering

Physically, peat smouldering vulnerability depends on three main soil properties: moisture content, bulk density, and mineral content. The moisture content distribution in peat layers has been shown to be the most important and controls the area and depth burned (e.g. Benscoter et al., 2011), based on the importance

of moisture content in ignition and spread of smouldering fire (Rein et al., 2008). Higher moisture levels inhibit smouldering because when moisture is present, the energy created in the combustion reaction is used to evaporate water rather than to continue combustion.

Bulk density is another factor influencing the vulnerability of peat to smouldering (Wilkinson et al., 2019). Peat with higher bulk density has more organic fuel per unit volume, which means that the peat will produce more energy when it ignites, thereby increasing the likelihood that peat smouldering can propagate laterally and or vertically (Benscoter et al., 2011; Wilkinson et al., 2019). The impacts of bulk density and moisture content on smouldering vulnerability are, however, not independent: Kohlenberg et al. (2018) found that a combination of bulk density, volumetric moisture content and a factor relating to the interaction of the two variables was best able to predict depth of burn (burn severity). Specifically, peat with higher bulk density was more vulnerable to deeper burning except for when the peat had high moisture content. Other variables (vegetation type or microtopography) did not improve depth of burn prediction (Kohlenberg et al., 2018).

Finally, peat with higher mineral content is less vulnerable to severe smouldering because the energy from the combustion is then used to heat up the minerals, which do not continue combustion, rather than other organic matter where the smouldering could continue (e.g. Hartford, 1993). Mineral content is also important for its relational impacts on peat smouldering: for example, if the peat has lower

mineral content, it is able to ignite (Frandsen, 1997) and smoulder (Huang et al., 2015) at higher levels of moisture. The depth of burn in a peat fire is controlled by moisture content and/or mineral content in that a smouldering fire will continue vertically downwards until it reaches mineral soil or significant moisture: a very wet layer (greater than 125% gravimetric moisture content) or otherwise wet conditions such as heavy rains (Rein, 2013).

Other peat properties such as the botanical or chemical composition of the peat (Cancellieri et al., 2012) and the physical structure of the peat - wherein matrix permeability, “cracks” in the peat surface, pores, or air channels impact the access to atmospheric oxygen which feeds smouldering (Rein, 2009, 2013) - also impact the smouldering process.

Peat depth and smouldering

While moisture content is the most important factor controlling the vulnerability of peat to deep smouldering, it would be difficult and impractical to map moisture content as it is quite dynamic: it changes through time depending on external factors such as precipitation and evapotranspiration, and peat properties like moisture retention and hydraulic conductivity (e.g., Waddington et al., 2015). In addition, moisture content varies vertically throughout the peat profile, and this vertical distribution is critical for smouldering propagation (Benscoter et al., 2011; Wilkinson et al., 2019). Other peat properties important for smouldering (bulk density and mineral content) also vary vertically within a peat profile and so to

accurately mapping them would require mapping multiple layers or multiple data points for a single location.

As the spatial (and temporal, for moisture) complexities of these peat properties make them difficult to leverage for mapping, a more temporally consistent and spatially simple proxy is needed. Conveniently, the relationship between peat depth and moisture content allows it to be used as a surrogate for moisture content when investigating vulnerability to high-severity peat smouldering (Moore et al., 2021; Wilkinson et al., 2020).

Briefly, deeper peatlands generally maintain a near-surface water table position longer during drought due to numerous autogenic ecohydrological feedbacks and the ecophysiological traits of peat moss (Wilkinson et al., 2020). *Sphagnum* mosses are integral to many peatlands, growing from the peat but also being decomposed into a main component of the peat material. *Sphagnum* mosses act as ecosystem engineers, creating the moisture conditions for their own success (Andrus, 1986; van Breemen, 1995). However, the feedbacks such as these, which enable peatlands to retain moisture, are less evident in shallower peatlands (Moore et al., 2021). Shallower peat deposits (with a confining layer such as bedrock below the peatland as is the case in the present study area) have been shown to be less able to retain moisture during long periods of high potential evaporation (Dixon et al., 2017). This is because there is less storage availability for water below the live *Sphagnum* – if there is less deep peat, and the layer below the peat cannot store water (because, in this case, it is impermeable), there is less water that the live

Sphagnum above the peat could potentially access (Dixon et al., 2017). Moreover, Moore et al (2021) surveyed peatlands during a summer drought and found that all shallow peatland sites (less than 40 cm) lost their water table while deep peatlands maintained a water table. The ability of peat to retain a water table has been posited as an important factor influencing peat smouldering vulnerability (Wilkinson et al., 2019). Because peatland depth can be used to identify vulnerability of *Sphagnum* to moisture stress (Moore et al., 2021), and peat moisture is a critical property in determining peatland vulnerability to fire, being able to map peat depths should enable better spatial understanding of peatland vulnerability to fire.

Nonetheless, moisture content is only one of several properties determining peat vulnerability to fire. The relationships between peat depth and bulk density or mineral content are also important when considering the utility of peat depth as a proxy for vulnerability to fire. Parry and Charman (2013) found that peat depth is strongly correlated with bulk density and mineral content in blanket bogs in the UK. However, there is not as much data on the relationship between bulk density and peat depth in boreal regions. Exploring that relationship will also enhance understanding of why peat depth mapping may be an effective tool for predicting peat vulnerability to smouldering.

Peat depth mapping

While a variety of methods have been used historically to map peat depths, they tend to either be too expensive or not precise enough to map a larger area (several km^2) at the scale of interest (1 m resolution).

The most basic method to determine peat depth is peat probe surveys, but these require considerable person-hours to map large areas. An alternative is ground penetrating radar (e.g. Parry et al., 2014), which is a geophysical technique that requires heavy equipment to be manually moved across the peatland surface to measure what is beneath the surface. Although both ground penetrating radar and peat probe surveys have high accuracies, they are very labour intensive and would be challenging to apply to areas greater than peatlands or small catchments, or areas that are particularly difficult to access. Electrical resistivity surveying and electromagnetic induction have also been used to map peatlands at the site level but again are fieldwork intensive (Minasny et al., 2019). Airborne electromagnetic induction (AEM) is another option that has been successful in thick peat depth mapping (e.g. Silvestri et al., 2019), however, using AEM alone can not accurately map thin peat layers (1-1.5 m) unless it is combined with extensive ground based electromagnetic surveying (Boaga et al., 2020).

Peat depths have also been mapped using airborne radiometric data. Examples of this include using potassium data at 100 m cell size sizes (Marchant, 2021), or using LiDAR (Light Detection and Ranging) data in combination with thorium, uranium and potassium radiometric data at a 10 m scale (Gatis et al., 2019). This method was not considered here as radiometric data in Canada is currently available only in specific areas and at 250 m resolution (Government of Canada, 2017).

For a much larger area, peat depths in Canada and the tropics have been mapped using open-access data and modelling (e.g. Minasny et al., 2020; Rudiyanto et al., 2018; Sothe et al., 2022). While this is very cost effective, these open-access data mapping projects tend to have pixel sizes of 30 m or more. This spatial resolution would not be effective for many small peatlands would be less than the size of one pixel, which is important as these small peatlands are at a higher risk of deep burning, as these small peatlands are generally shallower and in addition, margins of peatlands have very high vulnerability to fire as these small peatlands have a higher perimeter to area ratio (Lukenbach et al., 2015; Wilkinson et al., 2019).

Objectives

This thesis contains two data chapters. In the first, organic soil depth is mapped using machine learning and remote sensing. Given there are no other methods currently available to map peat depths with 1 m spatial resolution over landscape-sized areas efficiently and cost-effectively, this method provides a useful new tool. Improved peat depth mapping will have applications not only in peatland fire work as it is used here, but also many other uses, including improving species at risk habitat mapping, carbon storage accounting, and understanding peatland properties like greenhouse gas emissions or drought resistance (see Coulthard et al., 2009; Crezee et al., 2022; Markle et al., 2020; Moore et al., 2021).

The second data chapter further examines why mapping peat depth may be a useful tool for mapping peat depths by exploring the relationship between bulk density and peat depth. It expands on known relationships between peat properties

and smouldering vulnerability that exist in the literature (e.g., Frandsen, 1991; Lukenbach et al., 2015; Schulte et al., 2019; Wilkinson et al., 2020) by providing field-based data on how bulk density varies vertically within a peat profile.

Literature cited

Andrus, R. E. (1986). Some aspects of Sphagnum ecology. *Canadian Journal of Botany*, *64*(416–426).

Benscoter, B. W., Thompson, D. K., Waddington, J. M., Flannigan, M. D., Wotton, B. M., de Groot, W. J., & Turetsky, M. R. (2011). Interactive effects of vegetation, soil moisture and bulk density on depth of burning of thick organic soils. *International Journal of Wildland Fire*, *20*(3), 418–429. https://doi.org/10.1071/WF08183

Boaga, J., Viezzoli, A., Cassiani, G., Deidda, G. P., Tosi, L., & Silvestri, S. (2020). Resolving the thickness of peat deposits with contact-less electromagnetic methods: A case study in the Venice coastland. *Science of The Total Environment*, *737*, 139361. https://doi.org/10.1016/J.SCITOTENV.2020.139361

Cancellieri, D., Leroy-Cancellieri, V., Leoni, E., Simeoni, A., Kuzin, A. Y., Filkov, A. I., & Rein, G. (2012). Kinetic investigation on the smouldering combustion of boreal peat. *Fuel*, *93*, 479–485. https://doi.org/10.1016/J.FUEL.2011.09.052

Coulthard, T. J., Baird, A. J., Ramirez, J., & Waddington, J. M. (2009). *Methane Dynamics in Peat: Importance of Shallow Peats and a Novel Reduced-Complexity Approach for Modeling Ebullition*. https://doi.org/10.1029/2008GM000811

Crezee, B., Dargie, G. C., Ewango, C. E. N., Mitchard, E. T. A., Emba B, O., Kanyama T, J., Bola, P., Ndjango, J. B. N., Girkin, N. T., Bocko, Y. E., Ifo, S. A., Hubau, W., Seidensticker, D., Batumike, R., Imani, G., Cuní-Sanchez, A., Kiahtipes, C. A., Lebamba, J., Wotzka, H. P., … Lewis, S. L. (2022). Mapping peat thickness and carbon stocks of the central Congo Basin using field data. *Nature Geoscience 2022 15:8*, *15*(8), 639–644. https://doi.org/10.1038/s41561-022-00966-7

Dixon, S. J., Kettridge, N., Moore, P. A., Devito, K. J., Tilak, A. S., Petrone, R. M., Mendoza, C. A., & Waddington, J. M. (2017). Peat depth as a control on moss water availability under evaporative stress. *Hydrological Processes*, *31*(23), 4107–4121. https://doi.org/10.1002/hyp.11307

Frandsen, W. (1991). *Burning Rate of Smoldering Peat*. WSU Press. https://research.libraries.wsu.edu:8443/xmlui/handle/2376/1640

Frandsen, W. (1997). Ignition probability of organic soils. *Canadian Journal of Forest Research*, *27*(9), 1471–1477. https://agris.fao.org/agris-search/search.do?recordID=US201301792051

Gatis, N., Luscombe, D. J., Carless, D., Parry, L. E., Fyfe, R. M., Harrod, T. R., Brazier, R. E., & Anderson, K. (2019). Mapping upland peat depth using airborne radiometric and lidar survey data. *Geoderma*, *335*, 78–87. https://doi.org/10.1016/j.geoderma.2018.07.041

Government of Canada. (2017). *Canada - Radiometric survey data compilation - Open Government Portal*. https://open.canada.ca/data/en/dataset/289c931c-a1b1-55f8-8d93-4d88e66f1810

Hartford, R. A. (1993). *Smoldering combustion limits in peat as influenced by moisture mineral content and bulk density*. https://scholarworks.umt.edu/etd/7385

Huang, X., Rein, G., & Chen, H. (2015). Computational smoldering combustion: Predicting the roles of moisture and inert contents in peat wildfires. *Proceedings of the Combustion Institute*, *35*(3), 2673–2681. https://doi.org/10.1016/J.PROCI.2014.05.048

Kettridge, N., Humphrey, R. E., Smith, J. E., Lukenbach, M. C., Devito, K. J., Petrone, R. M., & Waddington, J. M. (2014). Burned and unburned peat water repellency: Implications for peatland evaporation following wildfire. *Journal of Hydrology*, *513*, 335–341. https://doi.org/10.1016/J.JHYDROL.2014.03.019

Kohlenberg, A. J., Turetsky, M. R., Thompson, D. K., Branfireun, B. A., & Mitchell, C. P. J. (2018). Controls on boreal peat combustion and resulting emissions of carbon and mercury. *Environmental Research Letters*, *13*(3), 035005. https://doi.org/10.1088/1748-9326/aa9ea8

Liu, J. C., Pereira, G., Uhl, S. A., Bravo, M. A., & Bell, M. L. (2015). A systematic review of the physical health impacts from non-occupational exposure to wildfire smoke. *Environmental Research*, *136*, 120–132. https://doi.org/10.1016/j.envres.2014.10.015

Lukenbach, M. C., Hokanson, K. J., Moore, P. A., Devito, K. J., Kettridge, N., Thompson, D. K., Wotton, B. M., Petrone, R. M., & Waddington, J. M. (2015). Hydrological controls on deep burning in a northern forested peatland. *Hydrological Processes*, *29*(18), 4114–4124. https://doi.org/10.1002/hyp.10440

Marchant, B. P. (2021). Using remote sensors to predict soil properties: Radiometry and peat depth in Dartmoor, UK. *Geoderma*, *403*, 115232. https://doi.org/10.1016/J.GEODERMA.2021.115232

Markle, C. E., North, T. D., Harris, L. I., Moore, P. A., & Waddington, J. M. (2020). Spatial Heterogeneity of Surface Topography in Peatlands: Assessing Overwintering Habitat Availability for the Eastern Massasauga Rattlesnake. *Wetlands*, *40*(6), 2337–2349. https://doi.org/10.1007/S13157-020-01378-2/FIGURES/6

Markle, C. E., Wilkinson, S. L., & Waddington, J. M. (2020). Initial Effects of Wildfire on Freshwater Turtle Nesting Habitat. *The Journal of Wildlife Management*, *84*(7), 1373–1383. https://doi.org/10.1002/jwmg.21921

Minasny, B., Berglund, Ö., Connolly, J., Hedley, C., de Vries, F., Gimona, A., Kempen, B., Kidd, D., Lilja, H., Malone, B., McBratney, A., Roudier, P., O'Rourke, S., Rudiyanto, Padarian, J., Poggio, L., ten Caten, A., Thompson, D., Tuve, C., & Widyatmanti, W. (2019). Digital mapping of peatlands – A critical review. *Earth-Science Reviews*, *196*, 102870. https://doi.org/10.1016/j.earscirev.2019.05.014

Minasny, B., Rudiyanto, Sulaeman, Y., & Setiawan, B. I. (2019). Open digital mapping for accurate assessment of tropical peatlands. In *Tropical Wetlands – Innovation in Mapping and Management* (pp. 3–8). CRC Press. https://doi.org/10.1201/9780429264467-1

Moore, P. A., Didemus, B. R., Furukawa, A., & Waddington, J. M. (2021). Peat depth as a control on Sphagnum moisture stress during seasonal drought. *Hydrological Processes*, *Press*. https://doi.org/10.1002/hyp.14117.

Ohlemiller, T. J. (1985). Modeling of smoldering combustion propagation. *Progress in Energy and Combustion Science*, *11*(4), 277–310. https://doi.org/10.1016/0360-1285(85)90004-8

Parry, L. E., & Charman, D. J. (2013). Modelling soil organic carbon distribution in blanket peatlands at a landscape scale. *Geoderma*, *211–212*(1), 75–84. https://doi.org/10.1016/j.geoderma.2013.07.006

Parry, L. E., West, L. J., Holden, J., & Chapman, P. J. (2014). Evaluating approaches for estimating peat depth. *Journal of Geophysical Research: Biogeosciences*, *119*(4), 567–576. https://doi.org/10.1002/2013JG002411

Rein, G. (2009). Smouldering Combustion Phenomena in Science and Technology. *International Review of Chemical Engineering*, *1*, 3–18. http://www.era.lib.ed.ac.uk/handle/1842/1152

Rein, G. (2013). Smouldering Fires and Natural Fuels. *Fire Phenomena and the Earth System: An Interdisciplinary Guide to Fire Science*, 15–33. https://doi.org/10.1002/9781118529539.CH2

Rein, G., Cleaver, N., Ashton, C., Pironi, P., & Torero, J. L. (2008). The severity of smouldering peat fires and damage to the forest soil. *Catena*, *74*(3), 304–309. https://doi.org/10.1016/j.catena.2008.05.008

Rudiyanto, Minasny, B., Setiawan, B. I., Saptomo, S. K., & McBratney, A. B. (2018). Open digital mapping as a cost-effective method for mapping peat thickness and assessing the carbon stock of tropical peatlands. *Geoderma*, *313*, 25–40. https://doi.org/10.1016/J.GEODERMA.2017.10.018

Schulte, M. L., McLaughlin, D. L., Wurster, F. C., Varner, J. M., Stewart, R. D., Aust, W. M., Jones, C. N., & Gile, B. (2019). Short- and long-term hydrologic controls on smouldering fire in wetland soils. *International Journal of Wildland Fire*, *28*(3), 177–186. https://doi.org/10.1071/WF18086

Silvestri, S., Christensen, C. W., Lysdahl, A. O. K., Anschütz, H., Pfaffhuber, A. A., & Viezzoli, A. (2019). Peatland Volume Mapping Over Resistive Substrates With Airborne Electromagnetic Technology. *Geophysical Research Letters*, *46*(12), 6459–6468. https://doi.org/10.1029/2019GL083025

Sothe, C., Gonsamo, A., Arabian, J., & Snider, J. (2022). Large scale mapping of soil organic carbon concentration with 3D machine learning and satellite observations. *Geoderma*, *405*, 115402. https://doi.org/10.1016/J.GEODERMA.2021.115402

Tarnocai, C. (2006). The effect of climate change on carbon in Canadian peatlands. *Global and Planetary Change*, *53*(4), 222–232. https://doi.org/10.1016/J.GLOPLACHA.2006.03.012

Turetsky, M. R., Benscoter, B., Page, S., Rein, G., Van Der Werf, G. R., & Watts, A. (2014). Global vulnerability of peatlands to fire and carbon loss. *Nature Geoscience 2015 8:1*, *8*(1), 11–14. https://doi.org/10.1038/ngeo2325

Turetsky, M., Wieder, K., Halsey, L., & Vitt, D. (2002). Current disturbance and the diminishing peatland carbon sink. *Geophysical Research Letters*, *29*(11), 1526. https://doi.org/10.1029/2001GL014000

van Breemen, N. (1995). How Sphagnum bogs down other plants. *Trends in Ecology & Evolution*, *10*(7), 270–275. https://doi.org/10.1016/0169-5347(95)90007-1

Waddington, J. M., Morris, P. J., Kettridge, N., Granath, G., Thompson, D. K., & Moore, P. A. (2015). Hydrological feedbacks in northern peatlands. *Ecohydrology*, *8*(1), 113–127. https://doi.org/10.1002/eco.1493

Wilkinson, S. L., Andersen, R., Moore, P. A., Davidson, S. J., Granath, G., & Waddington, J. M. (2023). Wildfire and degradation accelerate northern peatland carbon release. *Nature Climate Change 2023 13:5*, *13*(5), 456–461. https://doi.org/10.1038/s41558-023-01657-w

Wilkinson, S. L., Tekatch, A. M., Markle, C. E., Moore, P. A., & Waddington, J. M. (2020). Shallow peat is most vulnerable to high peat burn severity during wildfire. *Environmental Research Letters*, *15*(10), 104032. https://doi.org/10.1088/1748-9326/aba7e8

Wilkinson, S. L., Moore, P. A., & Waddington, J. M. (2019). Assessing Drivers of Cross-Scale Variability in Peat Smoldering Combustion Vulnerability in Forested Boreal Peatlands. *Frontiers in Forests and Global Change*, *2*, 84. https://doi.org/10.3389/ffgc.2019.00084

Chapter 2: Mapping Organic Soil Depths Across a Rock Barren, Forest, and Peatland Landscape

Background

Existing methods to map peat depth with an ~1 m resolution such as high-resolution manual mapping or using ground-penetrating radar require considerable intensive fieldwork and/or are expensive (Minasny et al., 2019). However, there is a need for high resolution peat depth maps because deeper peat areas are generally more vulnerable to smouldering due to the relationships between depth and bulk density, and depth and moisture content (Wilkinson et al., 2020). Improved peat depth mapping could also be beneficial for other applications, such as estimating landscape soil carbon storage (e.g., Gatis et al., 2019). Peat depth on the landscape isn't random, but rather depends on interconnected variables relating to topography, vegetation, and hydrology. Proxies of many of these variables can be mapped using remote sensing and GIS methods, therefore machine learning model approach is likely a good approach for high resolution mapping of peat depth. A forest-based classification and regression (also called "Random Forest") model not only can be used to produce a map but can also be used provide information about which GIS layers ("predictor variables") are most important in prediction, and therefore provide information about which ecohydrological variables might be most closely related to organic soil depth.

Mapping peat depth based on explanatory variables

Waddington et al. (2015) explain that peat depth is one of the critical variables that links numerous ecohydrological feedbacks that control peatland form and function. For example, the growth of the keystone moss species, *Sphagnum*, the expansion of shrubs on a peatland, peatland lateral drainage, evapotranspiration, water table sensitivity to drought, surface deformation and more are directly or indirectly controlled or related to peat depth. As mentioned above, peat depth on the landscape is not random, but rather controlled by landscape features and ecohydrological processes. This makes it an excellent candidate for mapping using a modelling method such as machine learning. A machine learning model can relate predictor variables (in this case, spatial data about landscape features) to training data (Maxwell et al., 2018). For example, field data like peat depth can be entered into a model with remotely sensed data to predict peat depths where there is remotely sensed data, but peat depths are unknown. As many of the variables highlighted as being linked to peat depth in Waddington et al. (2015) are topological, or have to do with above-ground vegetation, they are much easier to remotely sense than the belowground peat (e.g., Lopatin et al., 2019).

LiDAR data is widely used based on its ability to provide precise topographical information (Li et al., 2020). LiDAR can also be used to create GIS layers showing hydrological properties, such as the Topographic Wetness Index (TWI), an index used to predict moisture based on algorithms integrating slope and upstream contributing area of a pixel (Grimm et al., 2018). Other data related to properties

such as the location and height of individual trees or shrub density can also be obtained from LiDAR data (Campbell et al., 2018; Silva et al., 2022). Orthophotography can be used to create indices relating to vegetation health, water, and other landscape properties (e.g, Kriegler et al., 1969; McFeeters, 1996). Limiting a model to use only two data sources makes it more feasible to operationalize, especially with the current increasing availability of LiDAR and high-resolution orthophotography data, while still providing high-quality data that should be able to create an accurate model.

The objective of this chapter is to test to suitability of mapping organic soil depth using machine learning and remote sensing of an ~ 8 km^2 rock barren, forest and peatland landscape using LIDAR and 20-cm orthophotography from the Central Ontario Orthophotography Product (COOP) project.

Study area

The Dinner Lake study area is situated around 20 km north of Parry Sound, Ontario, Canada (45.457, -80.156), and is part of the Nibi (Water) Observatory for Boreal Ecohydrological Landscapes (NOBEL). The study area is within the Georgian Bay Biosphere Mnidoo Gamii, a UNESCO biosphere and is within the Robinson-Huron Treaty of 1850 and the Williams Treaty of 1923 and is located on Anishinabek territory.

The study area is located in a rock barrens and peatland landscape, part of the Boreal Shield ecozone (Markle et al., 2020; Moore et al., 2019). The granite rock

ridges (“barrens”) are situated between soil-filled, forested valleys. The barrens include mix of open rock, moss and lichen mats, peatlands, and ephemeral wetlands in depressions in the granite bedrock, and upland forest and juniper patches. The landscape has high heterogeneity, so mapping requires high spatial resolution. Landscape features such as small, forested peatlands often have considerable variability in peat depth within a few meters of space.

Methods

Field methods: test and training peat depth data

Organic soil depth was measured at 680 points across the Dinner Lake study area in the summer and fall of 2021. Peat depths were taken using a peat probe inserted vertically into the soil until bedrock or a “gritty” feeling indicative of mineral soil was reached. Prior to the field season, these sampling points were generated in square 3 x 3 grids of nine points (spaced 3 m apart) for ease of sampling. These grids were randomly selected across the study area, with the grids’ central points in approximately 50% peatlands, 25% forests and 25% moss mat or rock barrens, based on a pre-existing landcover classification. During the field season, landcover information was taken at the points to ensure the sampling points are balanced across the landscape types and because landcover type often varied within a 9-point grid.

Points were located with a Juniper Geode GNS2 for the high spatial accuracy needed to correlate the points with 1 m resolution remotely sensed data. Across 768 of the points taken using the Juniper Geode for this and other field data

collection, the average accuracy was 26.7 cm. Recorded accuracies ranged from 14.7 to 92.0 cm. Accuracy was worse in forested areas which had a mean accuracy of 34.5 cm compared to the sub-25 cm accuracies of all other land types (Figure 2.1). This high accuracy is important because this means points can be accurately tied to 1 m resolution remotely sensed data.

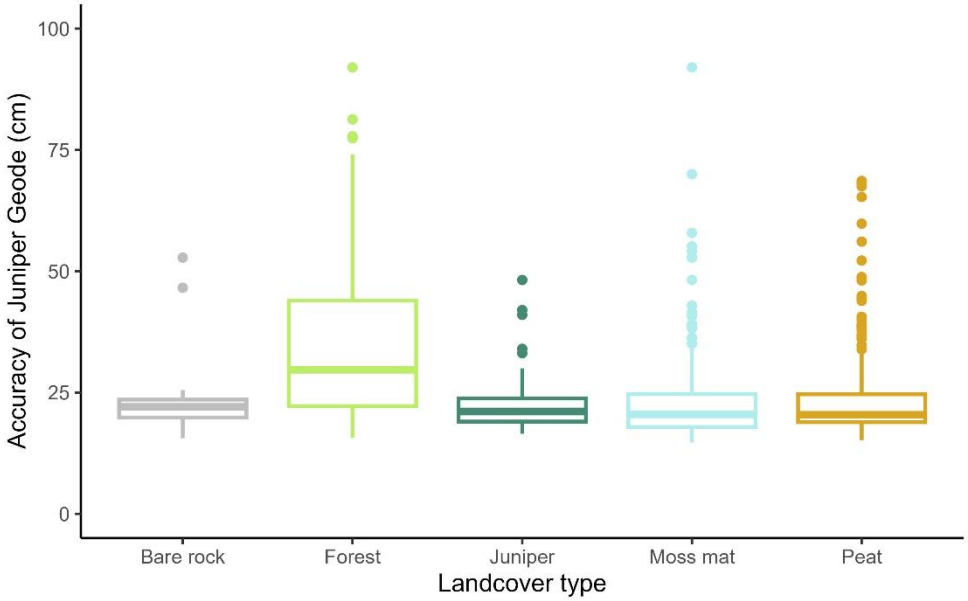

Figure 2.1: Spatial (horizontal) accuracy of the Juniper Geode by landcover type.

An additional 190 points were generated for open water and road (where ground truthing was infeasible due to highway traffic and water depths). These points were generated in 9-point grids with a randomly spaced center point from the landcover classification, and which were confirmed using COOP imagery and had peat depths classified as zero.

To increase the amount of training data points available to improve accuracy of the peat depth classification, further points from a pre-existing dataset of peat depths

were added to supplement the dataset. These peat depths were also highly spatially accurate as their locations were taken with a differential global positioning system. These peat depth surveys, which were also in grids with 3 m spacing, coved six peatlands of various sizes across the study areas (see Markle et al., 2020). In order to not unnecessarily skew the data to these peatlands, only 20% of the points available were used: an additional 513 points. This subset was taken from the dataset in random grids of 9 points to match the aforementioned methods.

Remotely sensed data

Two data sources, LiDAR data and high-resolution four-band COOP imagery were used for this project. Limiting this to two remotely sensed data sources allowed for simplicity and replicability at relatively cheaper costs, while still allowing for a large range of data layers to be created.

The COOP imagery has a 20 cm spatial resolution, with red, green, blue and near infrared bands, and was flown May 6th to June 10th, 2016. It is accurate to 50 cm on the ground at 90% (Ontario GeoHub, 2016). The LiDAR data used is not multispectral but does include intensity data which was used for the creation of some layers. The LiDAR data at Dinner Lake was flown Sept 30, 2019.

Model choice

While many modelling methods could be used for this project, a Random Forest model (RF, also called forest-based regression) machine learning method was chosen here for many reasons. To start with, RF is considered one of the top

machine learning methods in terms of accuracy (Maxwell et al., 2018). Forkuor et al. (2017) compared RF regression models to linear regressions and two other machine learning methods in high-resolution mapping of soil properties (note that these included SOC and clay content but not depth). The RF model most often had the highest accuracy both within the area the training data was from and also on additional verification outside of that area (Forkuor et al., 2017). This second part is important for a model to be operationalized efficiently. In addition, RF can be used for regression or classification (i.e., here it can be used to predict a range of peat depths rather than categorizing them, which allows for further usage of the peat depth map beyond fire). Finally, the RF model produces an output showing the importance of predictor variables. This means that knowledge is gained about which explanatory variables are most important. This is important because while feedbacks between the landscape features that are used as explanatory variables are understood to impact peat depth and therefore should be effective for the mapping outcome, there is no robust understanding of exactly which properties are most important for spatial variation in peat depth. The relative variable importance will provide a starting point to further examine this and potentially direct future studies on the topic.

The variable importance output of the RF model is also beneficial as the predictor variables used can be tested and optimized, though, generally, RF models are robust to dimensionality (i.e., the number of predictor variables used) and optimization, thereby requiring less work manipulating the model.

Pixel or polygon-based approaches are possible using an RF model; however, a pixel-based approach was used here as this makes most sense given the pixel-based input data and allows for the most precision.

As the RF algorithm is not spatial, it is important to have inputs that characterize the spatial relationships between the pixel and nearby elements (Poggio et al., 2019). Various methods such as smoothing, kriging and Euclidean distance fields can be used (Behrens et al., 2018; Poggio et al., 2019), but there are other ways to incorporate spatial elements too. Some predictor variables that are used here do this inherently (e.g., TWI is based on a flow accumulation algorithm and therefore incorporates data from the surrounding area). Incorporating nearby elements is also done in the present analysis through statistically summarising nearby cells, such as using an average in the 3 x 3 grid of cells surrounding the pixels. Using distance to the nearest object is also a method incorporated here, specifically distance to the nearest tree.

Validation and uncertainty analysis are both steps that should be done when mapping, but both are rarely done in peatland mapping (Minasny et al., 2019). Validation is done here using a 10% subset of points removed from the dataset while the model is run. Uncertainty estimation for RF models can be done in R (Lu and Hardin, 2021), but ArcGIS Pro also produces uncertainty outputs which will be used here. In this case, ArcGIS outputs layers showing minimum and maximum 90% confidence intervals of predicted depths.

Analysis and machine learning methods

All analysis was done in ArcGIS Pro unless otherwise indicated. Firstly, data layers were created from LiDAR and COOP remotely sensed data. These layers, which will be used as and referred to as "predictor variables," primarily correspond to one of the three overarching categories of topography, vegetation, and hydrology that occur on the landscape, and show these features in different ways or different scales or different subtypes. Layers were chosen for their relation with variables known to have feedbacks with peat depth, for example the shrub density layer was chosen as there is a known feedback between shrubification and peat depth (Waddington et al., 2015). They were also chosen based on the availability to produce a relevant and high-quality layer from the available COOP or LiDAR data.

Because RF is robust to autocorrelation of predictor variables, many similar predictor variable layers were created for some features as their similarity is not an issue for the analysis. Because various creation methods are available (for example, for TWI), this can also verify which version is the most useful predictor. LiDAR-derived layers have a cell size of 1 m as this was the minimum cell size that the point spacing of the LiDAR allowed for. COOP-derived products were aggregated from 0.2 m to 1 m after processing to match the resolution of the LiDAR-based layers. The abbreviated form of the predictor variable name used in figures is shown in parenthesis where applicable. A sample area of each predictor variable, as explained below, for reference is illustrated in Figure 2.2, along with the location of the study area within Ontario.

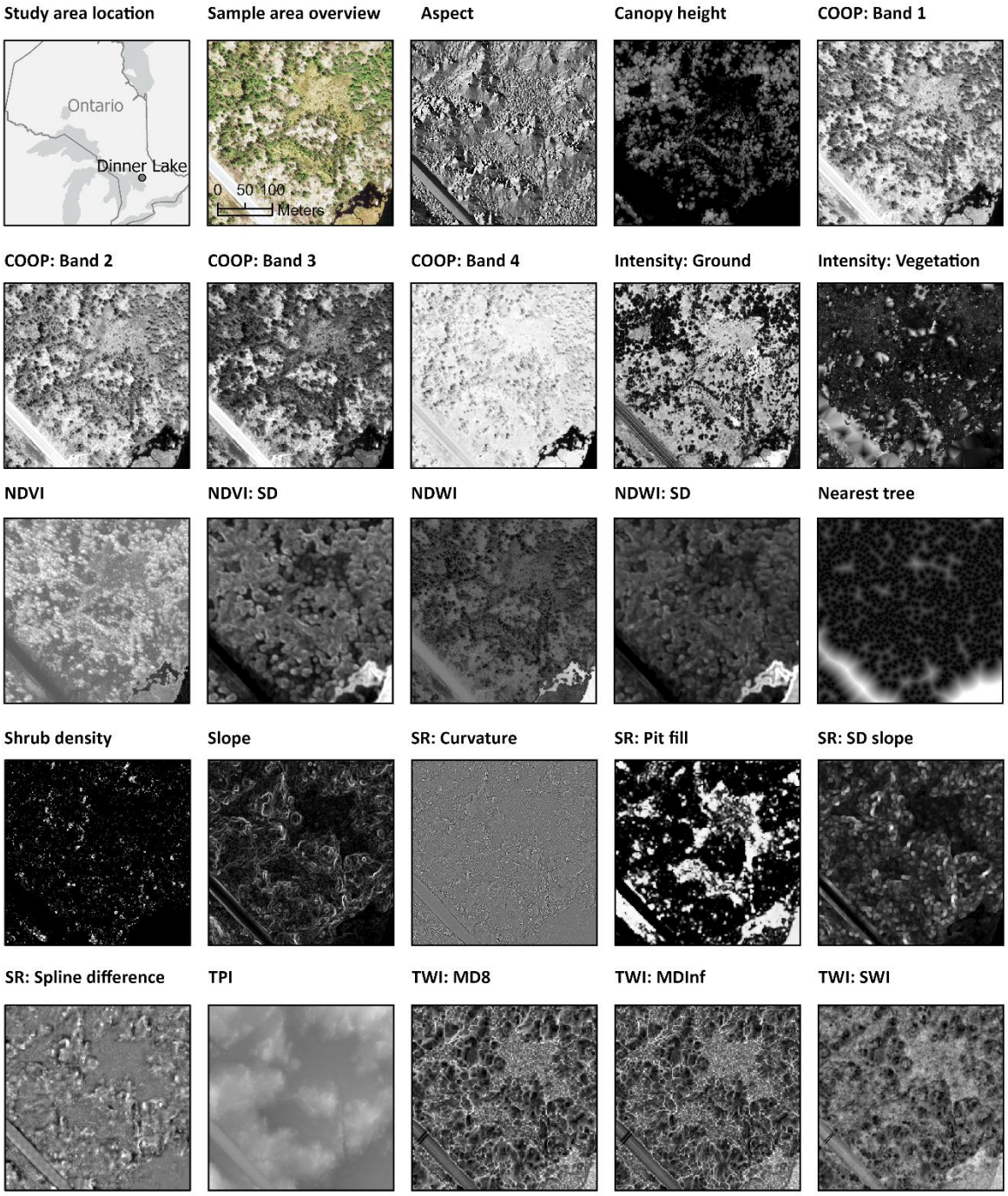

Figure 2.2: Predictor variable samples. This map includes a sample of all 23 predictor variables used in the model, as well as the study area location and COOP imagery showing the sample area containing forest, open rock, peatlands, water, and road.

Vegetation-related predictor variables

1. *Canopy height model (Canopy height).* Calculated as Digital Surface Model (DSM) – Digital Elevation Model (DEM). The DEM (which represents the ground surface) was developed using the triangulation method with linear interpolation and a 1 m pixel size of the points classified as ground. The DSM (which represents the height of objects in terrain such as treetops if there are trees or ground if there is no vegetation) used the same methodology as the DEM but for all non-noise points classified as first return. The DEM and DSM were initially included in the model but were not used in the final model as they consistently skewed the map. Though they generally improved the model numerically (i.e., the model had higher R^2 values when the DEM and DSM were included in runs), the resulting maps made with them were less accurate based on knowledge of the area. This is likely because nearby training data points had similar DEM or DSM values and similar peat depth values, but this is due to their spatial proximity rather than a particular mechanistic feedback from the DEM and DSM.
2. *Distance to nearest tree (Nearest tree).* Single tree point locations were generated from the canopy height model using Silva et al.'s 2022 tool using R. Distance raster was created in ArcGIS Pro using the Near tool.
3. *Shrub density.* The LiDAR dataset was classified by heights to get a dataset of points that were aboveground but less than or equal to 45 cm in heights, representing lower shrubs in peatlands. This height was chosen based on

examining average and maximum heights of shrubs from vegetation surveys done in the Dinner Lake area – generally, shrubs greater than 45 cm in height (but below the 1.37 m tree diameter at breast height cut-off) were in the forest, and peatland shrubs were less than 45 cm. The Point Statistics as Raster tool was used to get counts of the number of returns of a given height class per pixel. Shrub density (Campbell et al., 2018) was calculated as normalized relative point density by dividing the point counts of the aboveground to 45 cm category by the sum of that category plus lower (i.e. ground) points, to account for differences in returns caused by various factors such as tree canopies.

4. *Normalized Differential Vegetation Index (NDVI).* Calculated from COOP as (Near infrared (NIR) – red) / (NIR + red) (Kriegler et al., 1969).
5. *Standard Deviation of NDVI (NDVI: SD).* In order to have a metric that incorporates information relating to spatially adjacent cells of NDVI, the standard deviation of a specified radius was calculated for each pixel (e.g. Roger and Ramp, 2009; Tashakor et al., 2023). This method has been used to create predictor variables for models and has been considered to show variability or complexity of vegetation characteristics. Multiple radii were tested in model runs and a 20 m radius was found to be the best predictor of peat depth in this landscape at this scale.
6. *Average LiDAR Intensity – Above Ground (Intensity: Vegetation).* Donoghue et al., (2007) suggest that this is a useful predictor of tree genus proportion in a spruce and pine forest. Intensity for all above-ground points was extracted from

the LiDAR data using binning with linear interpolation to generate a layer with 1 m pixels. The intensity data was then normalized as intensity measurements vary between LiDAR flights and methods (Kashani et al., 2015).

Hydrological predictor variables

7. *Average LiDAR Intensity – Ground (Intensity: Ground).* Following Lang and McCarty (2009), this may present a measure of forest inundation. Intensity was extracted from the LiDAR data using binning with linear interpolation to a 1 m cell size. Intensity data was also normalized for this layer (Kashani et al., 2015).
8. *Normalized Differential Wetness Index (NDWI).* Calculated from COOP. Normally NDWI is considered to be calculated from NIR and short wave infrared bands, but because COOP does not have short wave infrared, an alternate method calculated as (green – NIR) / (green + NIR) was used (McFeeters, 1996).
9. *Standard Deviation of NDWI (NDWI: SD)*. For consistency, the same methods applied to spatialize the NDVI outlined above were used to create this layer. Again, multiple radii were tested in model runs and a 20 m radius was found to be the best predictor of peat depth in this landscape at this scale.
10. *TWI: Multidirectional flow algorithm (MD8, also known as FD8).* TWI is measure of predicted moisture based on algorithms integrating topographic factors: slope and upstream contributing area of a pixel. More than 10 algorithms for TWI exist, generally differing on the type of flow direction algorithm used. Three methods were chosen to be included here based on their utility in similar

landscapes and applications. MD8 is one of the most used algorithms, it performed best or near best in studies looking at different algorithms used for vegetation, soil moisture and soil pH in a variety of areas (Kopecký and Čížková, 2010; Raduła et al., 2018; Sørensen et al., 2006). For all TWIs, a DEM which was modified to allow flow paths though beaver dams and road and rail culverts was used. Sink-filling of the DEMs was not done as while some studies recommend it in their methodologies (e.g., Mattivi et al., 2019), it has also been shown to create "misleading" TWIs (Grimm et al., 2018), and it has also been argued that since depressions in DEMs are actual topographic features, they should be kept when making TWIs (Sørensen et al., 2006). While there is debate on appropriate pixel size for a DEM, a finer resolution is not always optimal however the spatial resolution should match the scale processes are happening at (Grimm et al., 2018). Based on expert knowledge of the area using a visual assessment of TWI results, the MD8 raster was created at 2 m (which was interpolated by the Random Forest model back to 1 m for the analysis). Tang et al. (2013) showed that different algorithm used in calculating slope from rasters have a significantly different results. Least squares was used for creating the slope raster for MD8; it was created in SAGA along with the flow accumulation rasters; raster calculator in ArcMap was used to create the final TWI:MD8 layer.

11. *TWI: MD Infinity or Triangular multiple flow direction (MDInf).* This algorithm outperformed similar algorithms such as the deterministic infinity algorithm in

studies (Kopecký and Čížková, 2010; Raduła et al., 2018; Rampi et al., 2014). It also outperformed the MD8 algorithm in two papers looking at identifying wetlands based on TWI (Grabs et al., 2009; Rampi et al., 2014) and for several variables (species richness, soil moisture and a wetness variable) in another study (Sørensen et al., 2006) in *Sphagnum* dominated wetlands in northern Sweden. The MD8 algorithm tends to be comparatively better for study areas similar to the present study area (i.e., areas with relatively gentle topography and wetlands) compared to mountainous areas. Similar to MD8, this TWI layer was created at a 2 m spatial resolution, using SAGA to create the slope raster (least squares method) and flow accumulation grid, raster calculator in ArcMap was used to create the TWIs.

12. *TWI: The SAGA Wetness Index (SWI).* This method uses the MD8 algorithm, but has a modified calculation which was created to improve performance in flatter areas (Böhner and Selige, 2006; Böhner et al., 2002). Default suction (10) and area (square root catchment area) were used. SWI uses a catchment slope method, was created at a 1 m resolution, and was done entirely in SAGA. SWI has been used successfully a boreal forest landscape (Andersson, 2009).

Topographical predictor variables

13. *Slope.* From DEM, calculated using the default least squares algorithm in degrees.
14. *Aspect.* From DEM. Aspect was included as it has been shown to be a main control on peat depth (Cao et al., 2017).

15. *Topographic Position Index (TPI).* The Focal Statistics tool was used to calculate the mean elevation around each cell within an annulus window with a center radius of 1 m, and an outer radius of 200 m. The TPI value was calculated by subtracting the mean neighbourhood elevation of each cell from the elevation of that cell. The 200 m radius was chosen as it optimized during separate modelling study in a similar area; a 200 m radius was found to minimize noise while identifying peat-filled depressions (Tekatch et al., *in press*).
16. *Standard Deviation of Slope (SR: SD slope).* This is one of four methods of measuring surface roughness proposed by Brubaker et al. (2013). It was calculated from the slope layer using Focal Statistics with a 5 m x 5 m moving window.
17. *Pit fill (SR: Pit fill).* Another Brubaker et al. (2013) method, here a filled/hydrologically corrected DEM was subtracted from the DEM. The average from a 3 m x 3 m surrounding area was calculated using Focal Statistics.
18. *Standard Deviation of Residual Topography (SR: Spline difference).* A third Brubaker et al. (2013) method for mapping surface roughness, here the DEM was thinned to 10 m resolution using resample with the bilinear resampling technique. A regularized spline with a weight of zero was constructed for the 10 m resolution data (which had been converted into points), and then the spline was interpolated to a 1 m resolution. Finally, the original DEM was subtracted

from the interpolated spline to get a result showing the difference between the actual topography and the broader area topography as mapped by the spline.

19. *Standard Deviation of Curvature (SR: Curvature).* For the final Brubaker et. al. (2013) method, curvature was calculated in SAGA using the Zevenbergen and Thorne method, and then focal statistics was used to find the standard deviation over a 5 m moving window.

Additional predictor variables

20. *COOP band 1.* Red. While COOP band data does not directly relate to an ecohydrological variable, all four available bands were included as they are readily available and provide additional information the model may be able to use.
21. *COOP band 2.* Green.
22. *COOP band 3*. Blue.
23. *COOP band 4*. NIR.

These 23 layers were put into RF machine learning model with the peat depths as the variable to predict. Environment settings were set to defaults except 0% of training data was excluded for validation. This is because a 10% subset of the training data (139 points) was manually removed before running the model; these were separated out by grid so that the potential closeness and similarity of the points wasn't creating a spatial autocorrelation issue. One hundred percent of data was available per tree, there were 20 runs for validation, and the number of trees

was increased to 500. Uncertainty calculation was done wherein rasters with minimum and maximum peat depth of 90% certainty were created.

Results and Discussion

Peat depth map

The main result of this section is the production of a peat depth map (Figure 2.3). Based on general knowledge of the area from fieldwork, these results are visually accurate. Areas known from familiarity with the study areas to be peatlands are consistently the deepest areas, with deeper peat depths closer to the center of peatlands, as expected. The model identifies known small and forested peatlands as well. Forested areas have higher peat depths than bare rock areas (as expected – the model treats organic soil in the forest the same way as peat in peatlands). For example, forested valleys are evident on the map. Lakes and roads are near zero as expected. An evident issue where floating mats are mapped as deeper than they should be, however this is likely due to having no training data on floating mats as they are difficult to access.

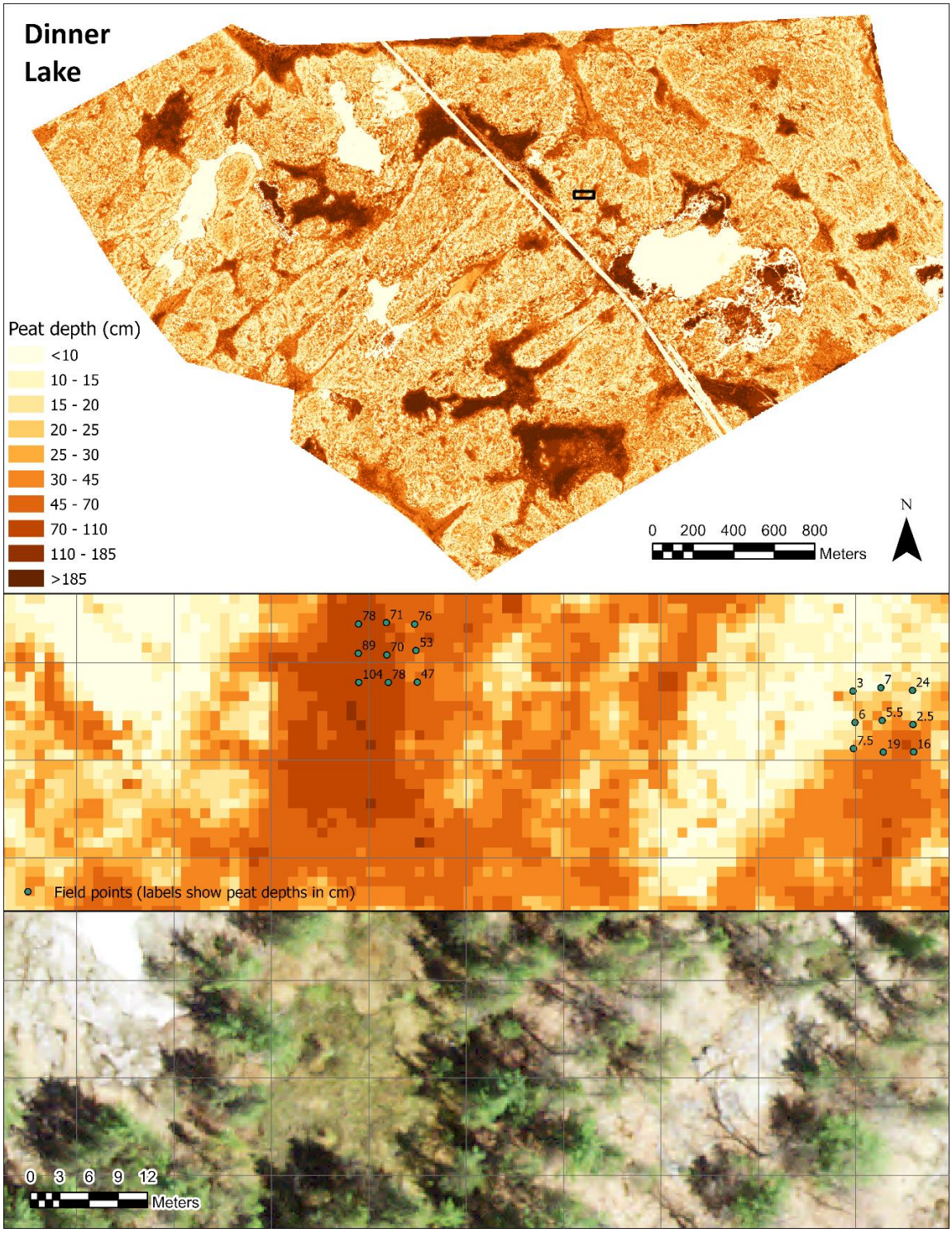

Figure 2.3: Modelled peat depth at Dinner Lake. The top panel shows the entire mapped area. The bottom two panels show detail of the area marked by the black box on the top panel. The middle panel shows the peat depth model along with two 'grids' of field data points: peat depths from these points were used in the creation of the model. The final panel shows COOP imagery. Because COOP was taken during leaf off, deciduous forest areas are hard to discern in the image.

Model accuracy and uncertainty

The default metric used to assess the model in ArcGIS is the R^2 value, which for the 10% of points removed for testing was 0.73, which is a good fit for an environmental model. However, other metrics more commonly used in evaluating mapping did not have as successful results: the Route Mean Squared Error (RMSE) was relatively high (36 cm) as was the Mean Absolute Error (MAE), at 28 cm. These error values may be high due to the relatively low number of test points used (10% of total points for a total of 139), and the difficulty in mapping this belowground variable using optical and above-ground remotely sensed data. Furthermore, to eliminate the possibility of spatial autocorrelation artificially inflating model accuracy, these 139 points are only from a small number of 9-point grids. If test points from the same grids as those used to train the model, the potential similar properties in the predict tor variables and peat depth of adjacent points might have allowed for artificially improved model results. However, given that there were only a few small areas used for testing, if some of these test point grids were in areas that behaved atypically, this would greatly worsen the accuracy results. Despite the relatively high RMSE and MAE values, a visual assessment of the map matches known peat and organic soil depth trends in the area, suggesting that this is still a useful product.

Examining the actual and predicted values from the 139 test points, the model tends to overpredict peat depths in shallow areas and underpredict peat depths in deeper areas (Figure 2.4). This shows why the R^2 value indicates improved

predictor power compared to the MAE and RMSE: the R^2 value is not tied to a 1:1 relationship between actual and modelled depths as the MAE and RMSE are.

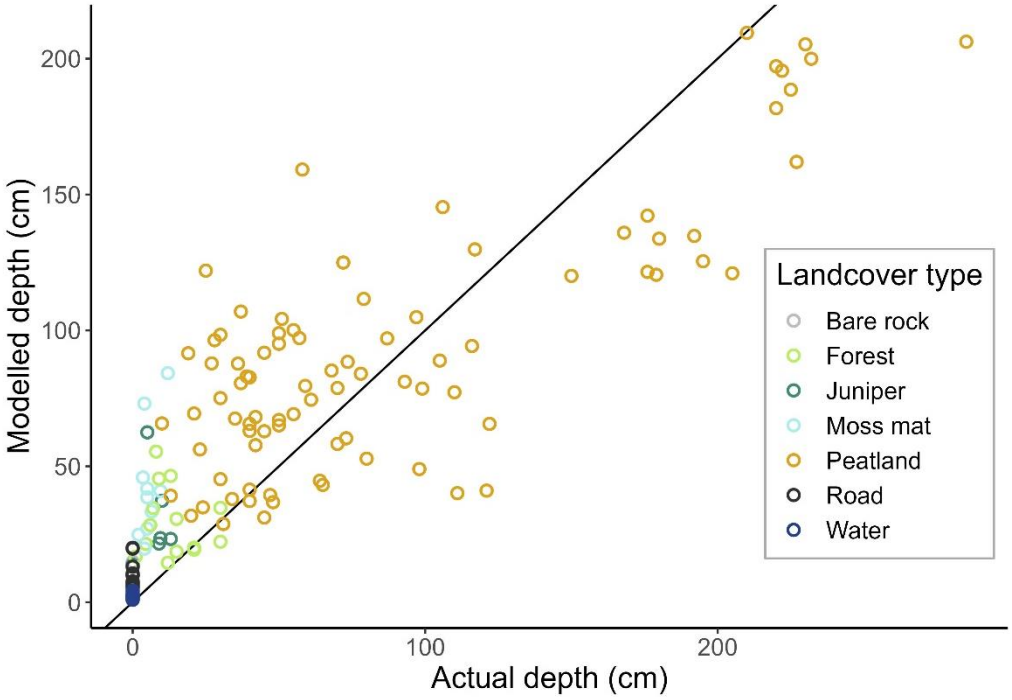

Figure 2.4: Modelled peat or organic soil depth compared to actual depth at test points. The black line shows where equal modelled and predicted values would be.

As always in modelling, to reduce uncertainty, increasing the number of training datapoints may help improve model accuracy; this study was limited by COVID-19 field research access restrictions. Nevertheless, including a large number of training points was favoured over increasing the number of test data points despite the possible negative impacts on numeric assessments of accuracy. Other methods to improve the model such as changing the number of trees and other model parameters, and changing which remotely sensed data layers were used, were tested repeatedly throughout the model creation process.

Another method of assessing the present model results is the uncertainty values produced by the ArcGIS Pro tool. The model produced 90% certainty intervals showing a high and low range of potential peat depth values. Subtracting the low from the high values gives a range that could be considered a metric of model accuracy that can be mapped across the landscape (Figure 2.5). While this gives very large ranges (up to 382 cm between the lower and upper predictions for some areas), the prediction range will be considered here as a relative measure of model efficacy rather than focusing on the exact numbers. In Figure 2.5, areas with high uncertainty are shown in dark and areas with low uncertainty ranges are in light.

The map reveals some interesting patterns in the variation in uncertainty ranges. One notable pattern here is that uncertainty is extremely high in floating peat mats. This is likely because these features were not included in the training data as sampling them was infeasible. Since there are no field data points of similar features to compare to, it forces the model to extrapolate, which is not a strength of RF models. Specifically, here the model would not be extrapolating from a range of peat depths, as most of the depths of floating mats would be within the sampled peat depth range, but rather the combination of explanatory variables from these floating mats are likely not found within the training data points. As floating mats are unlikely to burn in a wildfire because they're on lakes that are relatively unlikely to dry out, the peat map uncertainty is less of an issue for this intended use.

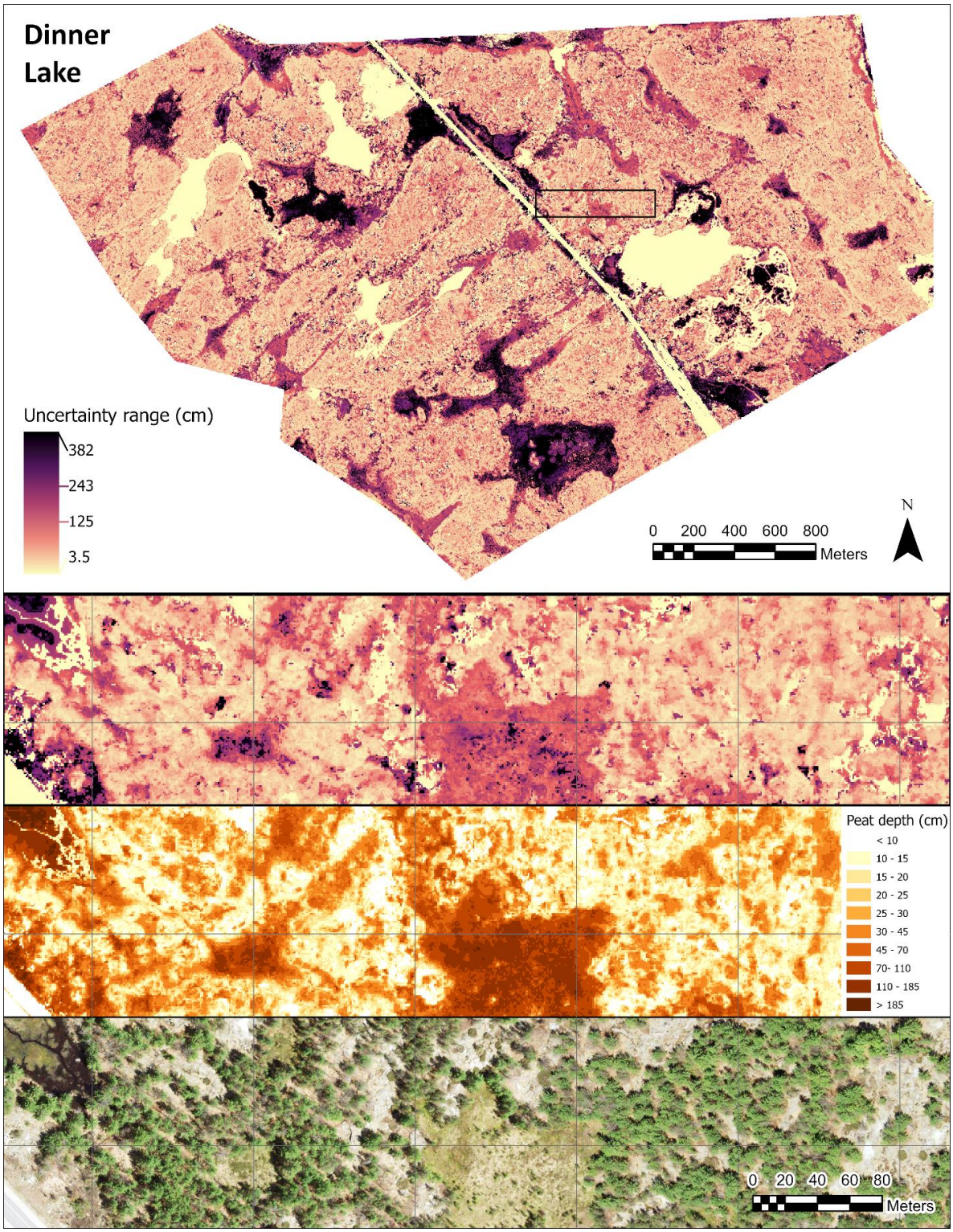

Figure 2.5: Uncertainty in peat depth model at Dinner Lake. The top panel shows the entire mapped area. The bottom three panels show detail of the area marked by the black box on the top panel. The topmost detail panel shows the uncertainty of the peat depth model, the middle shows peat depth, and the final panel shows COOP imagery for the same area.

The other landcover type where uncertainty is high is within the middles of large peatlands, which is to be expected as there is a large range in possible depths there and compared to shallower areas, it is relatively hard to predict based on surface features. For example, none of the predictor variables used here account for the shape of the underlying bedrock, which would be challenging to obtain data for. Additionally, it is likely that deeper peat depths have fewer impacts on peatland surfaces processes such as tree growth and microtopography formation (see Waddington et al., 2015) which are included in the predictor variables. Uncertainty in these deeper peatlands is high despite the training points used in the model being weighted heavily towards peatlands (Figure 2.6). Again, this is less of an issue if the peat depth model is being used for wildfire vulnerability mapping, as middles of peatlands are not as vulnerable to severe smouldering as margins (Wilkinson et al., 2020).

A further method of testing this model would be to apply the same model to a different study area with more peat depth test data points. This was an intended to be done at an area adjacent to the 2018 PS33 fire using pre-fire LiDAR and COOP data. If sufficiently accurate, the model could then be applied the burned area, which could be compared to burn depths calculated by the difference in the DEMs of pre- and post-fire LiDAR (Mickler et al., 2017). Unfortunately, a data availability issue prevented this analysis.

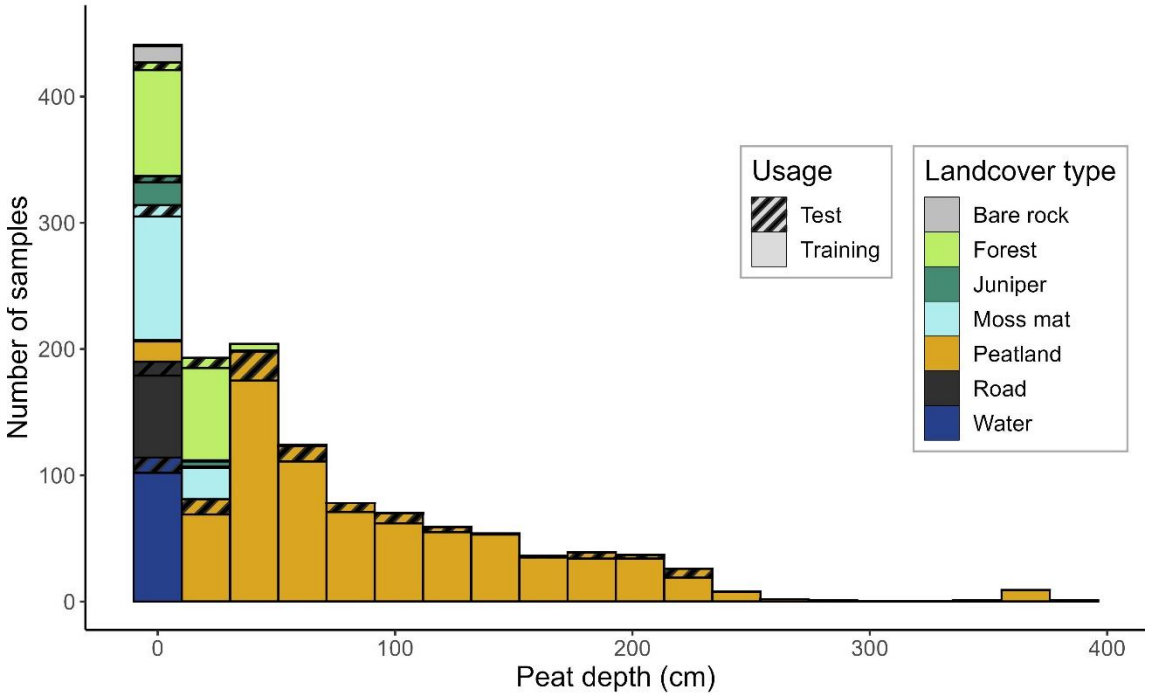

Figure 2.6: Test and training data by land type and peat depth.

Relative importance of predictor variables

The model also provides the relative importance of each predictor variable as an output (Figure 2.7). This plot shows the 'importance' of each input predictor variable to the final model of each of the 20 model runs. Because most of the predictor variables are tied to landscape elements such as hydrology, vegetation, or topography, inferences can be made from the importance as a predictor of these variables to their relationship with peat depth on the landscape either from how that feature impacts peat depth or how peat depth impacts that variable. While higher importance values mean they have a higher impact on the prediction,

correlation between layers, while it does not negatively impact the model itself, may impact the relative importance of the correlated variables (Strobl et al., 2008).

No particular variable type (hydrology, topography, or vegetation) or source (LiDAR or COOP) stands out as having particularly high importance, as might be expected given the known links between peat depth and all of these variables.

The following analysis considers the predictor variables by importance. The variable with the highest importance was TPI. TPI may have the highest importance because generally the higher up rock ridges have shallow peat/organic soil depths, and peatlands and forested areas with slightly thicker organic soils are positioned in topographically lower areas. Figure 2.8 shows the relationship between each predictor variable and peat depths at all training and test points. The TPI- peat depth relationship is particularly interesting given the multimodal distribution of the TPI.

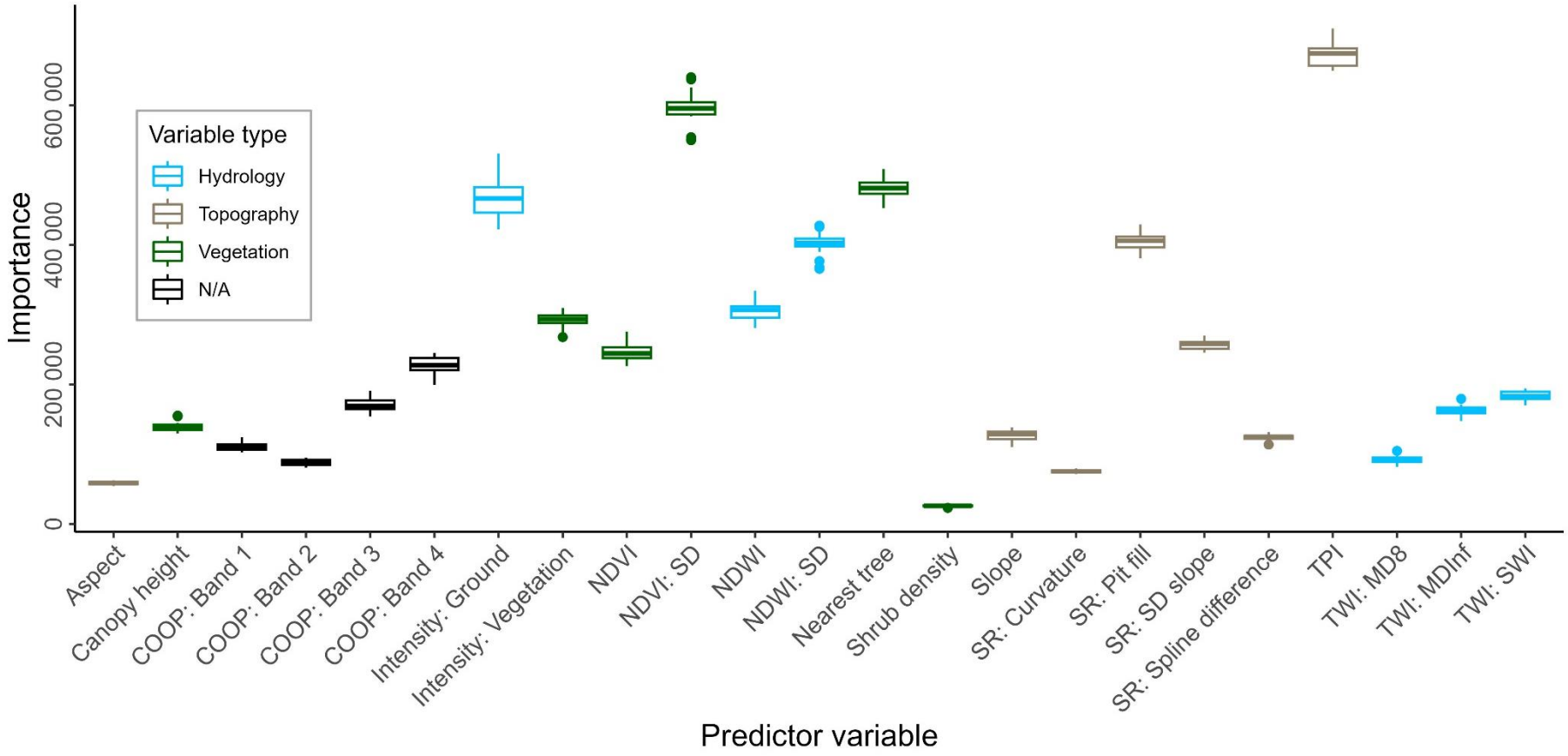

Figure 2.7: Relative importance of predictor variables as calculated by ArcGIS Pro. Includes data from the 20 runs done by the model.

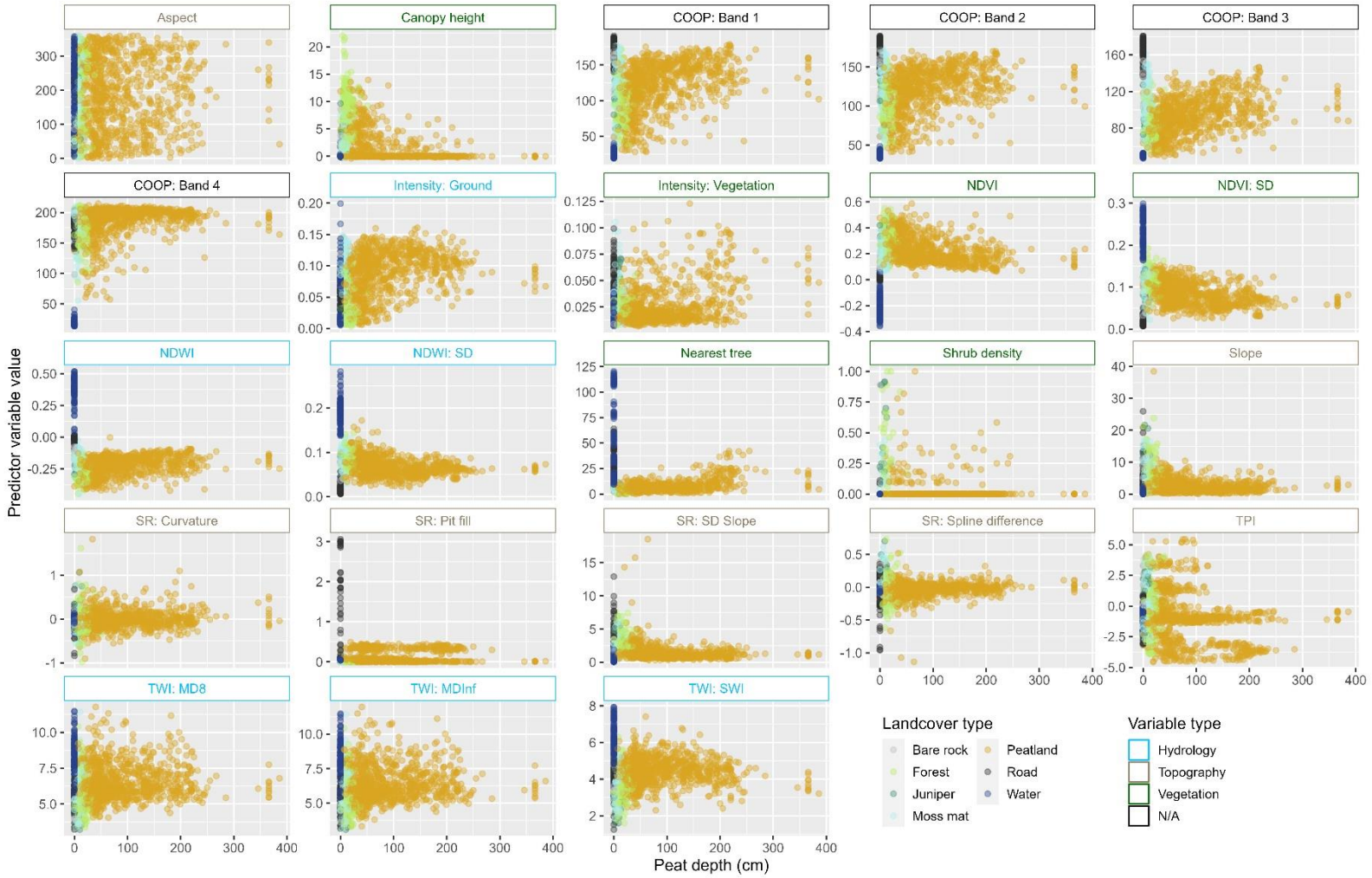

Figure 2.8: Predictor variable relationships with peat depth at all test and training points. Points are coloured by landcover type and subplot title color indicates the type of predictor variable.

The second highest variable importance is that of the NDVI: SD layer, which is a metric of vegetation complexity within a 20 m radius of the pixel. This metric is likely able to differentiate between different land cover classes based on homogeneity; looking at this layer is clearly very low on roads, low in peatlands (especially closer to the middles), higher in forests, and highest around the edges of lakes (where the very different NDVI values in the water and surrounding vegetation are included in the standard deviation). By representing the difference between landcover types, it can differentiate peat depths as they are related. In addition, because of the edge effects between landcover types, it may inadvertently produce similar patterns to peat depths as peat is often deeper towards the middle of the peatlands, where the NDVI: SD is lower.

The distance to the nearest tree also was a very important predictor. This again seems to group values by landcover type well (for example, values are generally low in forested areas, but higher in lakes). But there may be an important relationship within peatlands as well. In the open peatlands, distance from nearest tree increases from the forested edge of peatlands inwards, which should correlate with deeper peat depths as they tend to be deeper in the center given a bowl shape of underlying bedrock, and as generally found by peatland depth transects taken in this study area. Another important, function-based factor is distance from trees within peatlands. Based on field observations, peat depths adjacent to trees were generally shallower than ones further away. This is supported by other analysis:

Markle et al. (2020) found that trees tended to be found where peat depth shallower than average.

The next most important factor is ground intensity, which is a measure of forest inundation. This may be correlated to peat depths, as deeper peatlands retain water tables better (Moore et al., 2021). Similarly, organic soil in forests or moss mats might be more likely to be moist than bare rock. A consideration for this predictor variable is that it may increase error in applying the model to other locations if the LiDAR was flown at a different time of year, given annual variability in moisture. NDWI: SD was also a relatively important predictor, likely due to similar reasons, though it does not sense through to the ground and is primarily effective at identifying lakes.

Of the surface roughness metrics, the Pit fill predictor variable was the most important. This may again be because it distinguishes between landcover types as can be seen in Figure 2.5, however it is possible this also picks up on microtopography: in this landscape, peatlands generally having flat expanses that are undular with hummocks and hollows. This can be contrasted with considerably sloping forest valleys or the flat rock ridges. Furthermore, given the feedbacks wherein peat depths determine water table levels, which impact vegetation factors like moss growth and decay and therefor hummock-hollow production (Nungesser, 2003), microtopography depths in peatlands should also be correlated to peat depths. Field observation suggests deeper peatlands have larger hummock heights.

All COOP bands, all TWIs, shrub density, and many topography layers such as slope, aspect, and some surface roughness metrics were all relatively unimportant. While this may be due to the aforementioned impacts of correlated variables, there are some explanations that can provide insight when developing future models. For example, the vegetation Intensity layer may have outperformed NDVI because deciduous trees are easily discernable from the LiDAR compared to in the leaf-off COOP data, and in addition there are no shadow effects since LiDAR is an active sensor. The shrub density layer had the lowest variable importance – this may be because it is not a constant raster in a sense that there are a lot of zero-values because there's no returns at the defined shrub height for many pixels. One detriment of TWI is it imagines the landscape through flow generation, which although this may be accurate in many steeper, less permeable landscapes, does not accurately reflect hydrological processes in this landscape; while the chosen algorithms allow for multi-directional flow and should be better in terms of this (Lang and McCarty, 2009), it may still be an issue.

Spatial arrangement of peat depth ranges for wildfire applications

For an analysis of which areas are most vulnerable to fire and their patterns across the landscape, the peat depths as predicted by the model were categorized into four categories: 0 - 20 cm, 20 - 40 cm, 40 - 66 cm, > 66 cm. These categories were chosen because 66 cm is the breakpoint found by Wilkinson et. al. (2020) wherein deeper peat is less vulnerable to deep burning in smouldering fire, 40 cm is the minimum peat depth for peatlands in Canada (National Wetlands Working Group,

1997), and the 20 cm cutoff was chosen to categorise areas with relatively shallow layers of soil, given the error level in the model and its overprediction of areas with lower peat depths. Across the landscape, 38% of the area had organic soil from 0 - 20 cm in depth, 33% of the area had 20 - 40 cm depth, 14% of the area had 40 - 66 cm depths, and 14% of the area had peat depths greater than 66 cm. Visually, the highest category of depths is constrained to large peatland areas, along with road, water, and bare rock areas in the 0 - 20 cm depth range. The intermediate categories were particularly interesting, with the 20 - 40 cm and 40 - 66 cm depths scattered across the landscape. To numerically demonstrate this, pixels were grouped together by category to form patches of adjacent pixels in the same category, and these patches were classified by area (Figure 2.9).

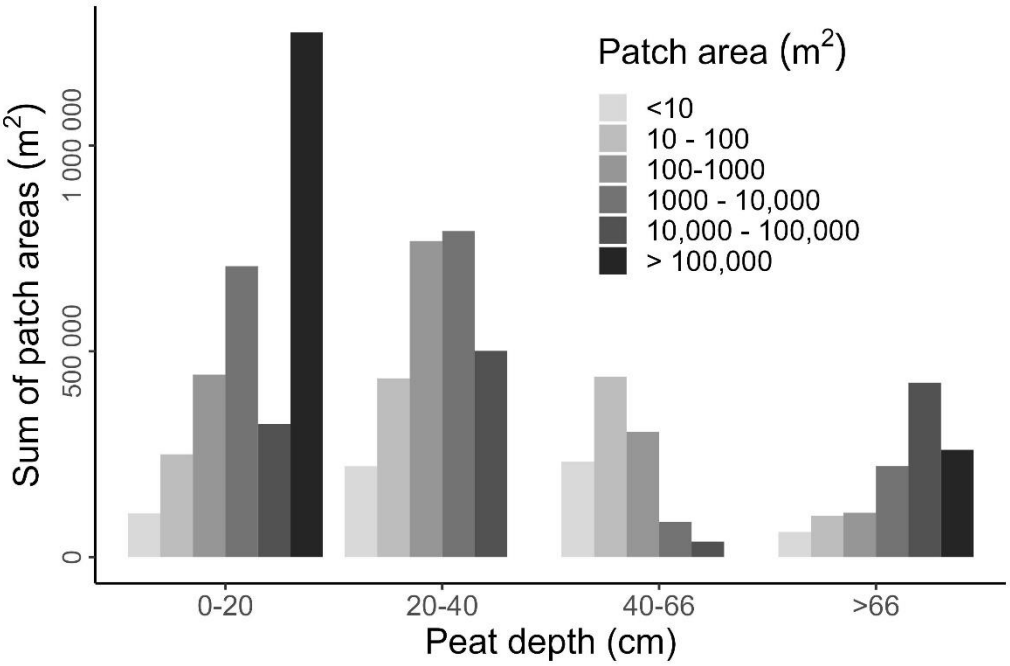

Figure 2.9: Total area of landscape segments divided by modelled peat depths, as categorized by patch area.

In this analysis, the large area of highly connected low-peat depth (0-20 cm) patches are lakes and the road in the study area. Note that this analysis would include margins of a deeper peatland in the same category as a same-depth smaller peatland.

Figure 2.9 demonstrates that while the majority of deep peat (> 66 cm) can be found in large continuous areas, peats in the 20 - 40 and 40 - 66 cm depth ranges were predominantly in small (10 - 1000 m^2) patches. This may be impacted in part by the category cut-off values and lower peat depth areas within the 40 - 66 cm category, for example, however does demonstrate the evident factor of these 40 - 66 cm peat depth areas, which both are a) vulnerable to deep burning because they are < 66 cm in depth and b) liable to burn more peat given there is more peat available to be burned, are not in easy to find or manage patches of the landscape but rather distributed across.

The large, deep peatlands are still important to consider, however, as they may act as wildfire refugia, providing undisturbed habitat for animal and plant species during and after fires (Tekatch et al., *in press*).

Conclusion

This project presents an effective method to map peat depths at a 1 m spatial resolution in a complex landscape using just two readily available datasets. The most important predictor variables ranged across the categories of hydrology, vegetation, and topography, likely based on various ecosystem feedbacks.

The final peat depth map shows intermediate peat depths (areas that are deep enough that there is a significant volume of peat that can smoulder and release carbon to the atmosphere, but not so deep that the peatlands will retain their water table during most droughts and therefore not as vulnerable to fire) are not grouped together but rather scattered across the landscape in patches. This type of landscape may, therefore, provide added challenges for fire managers. Scattered small smouldering areas across a landscape may be harder to restore or otherwise protect from wildfire, compared to specific large peatlands. In addition, these areas may be more difficult to find without more complex methods such as the one prevented here (as they are often forested or less obvious on satellite imagery compared to large distinct peatlands). As such, methods such as the one presented here may be key for fire managers to better understand the landscape and to improve potential for increased resiliency.

Literature cited

Andersson, J.-O. (2009). A GIS-based landscape analysis of dissolved organic carbon in boreal headwater streams. In *Karlstad University Studies*. www.kau.se

Behrens, T., Schmidt, K., Viscarra Rossel, R. A., Gries, P., Scholten, T., & MacMillan, R. A. (2018). Spatial modelling with Euclidean distance fields and machine learning. *European Journal of Soil Science*, *69*(5), 757–770. https://doi.org/10.1111/ejss.12687

Böhner, J., & Selige, T. (2006). Spatial prediction of soil attributes using terrain analysis and climate regionalisation. *SAGA - Analysis and Modelling Applications*, *115*, 13–27. https://doi.org/10.1186/1471-2288-4-5

Böhner J, Köthe R, Conrad O, Gross J, Ringeler A, & Selige T. (2002). *Soil regionalisation by means of terrain analysis and process parameterisation*.

Brubaker, K. M., Myers, W. L., Drohan, P. J., Miller, D. A., & Boyer, E. W. (2013). The use of LiDAR terrain data in characterizing surface roughness and microtopography. *Applied and Environmental Soil Science*, *2013*. https://doi.org/10.1155/2013/891534

Campbell, M. J., Dennison, P. E., Hudak, A. T., Parham, L. M., & Butler, B. W. (2018). *Quantifying understory vegetation density using small-footprint airborne lidar*. https://doi.org/10.1016/j.rse.2018.06.023

Cao, B., Gruber, S., Zhang, T., Li, L., Peng, X., Wang, K., Zheng, L., Shao, W., & Guo, H. (2017). Spatial variability of active layer thickness detected by ground-penetrating radar in the Qilian Mountains, Western China. *Journal of Geophysical Research: Earth Surface*, *122*(3), 574–591. https://doi.org/10.1002/2016JF004018

Donoghue, D. N. M., Watt, P. J., Cox, N. J., & Wilson, J. (2007). Remote sensing of species mixtures in conifer plantations using LiDAR height and intensity data. *Remote Sensing of Environment*, *110*(4), 509–522. https://doi.org/10.1016/J.RSE.2007.02.032

Forkuor, G., Hounkpatin, O. K. L., Welp, G., & Thiel, M. (2017). High Resolution Mapping of Soil Properties Using Remote Sensing Variables in South-Western Burkina Faso: A Comparison of Machine Learning and Multiple Linear Regression Models. *PLOS ONE*, *12*(1), e0170478. https://doi.org/10.1371/JOURNAL.PONE.0170478

Gatis, N., Luscombe, D. J., Carless, D., Parry, L. E., Fyfe, R. M., Harrod, T. R., Brazier, R. E., & Anderson, K. (2019). Mapping upland peat depth using airborne radiometric and lidar survey data. *Geoderma*, *335*, 78–87. https://doi.org/10.1016/j.geoderma.2018.07.041

Grabs, T., Seibert, J., Bishop, K., & Laudon, H. (2009). Modeling spatial patterns of saturated areas: A comparison of the topographic wetness index and a dynamic distributed model. *Journal of Hydrology*, *373*(1–2), 15–23. https://doi.org/10.1016/j.jhydrol.2009.03.031

Grimm, K., Nasab, M. T., & Chu, X. (2018). TWI computations and topographic analysis of depression-dominated surfaces. *Water (Switzerland)*, *10*(5). https://doi.org/10.3390/w10050663

National Wetlands Working Group. (1997). *The Canadian Wetland Classification Scheme*. 1–67.

Kashani, A. G., Olsen, M. J., Parrish, C. E., & Wilson, N. (2015). A Review of LIDAR Radiometric Processing: From Ad Hoc Intensity Correction to Rigorous Radiometric Calibration. *Sensors 2015, Vol. 15, Pages 28099-28128*, *15*(11), 28099–28128. https://doi.org/10.3390/S151128099

Kopecký, M., & Čížková, Š. (2010). Using topographic wetness index in vegetation ecology: does the algorithm matter? *Applied Vegetation Science*, *13*(4), 450–459. https://doi.org/10.1111/j.1654-109X.2010.01083.x

Kriegler, F., Malila, W., Nalepka, R., & Richardson, W. (1969). *Preprocessing Transformations and Their Effects on Multispectral Recognition*.

Lang, M. W., & McCarty, G. W. (2009). Lidar Intensity for Improved Detection of Inundation Below the Forest Canopy. *WETLANDS*, *29*(4), 1166–1178.

Li, X., Liu, C., Wang, Z., Xie, X., Li, D., & Xu, L. (2020). Airborne LiDAR: state-of-the-art of system design, technology and application. *Measurement Science and Technology*, *32*(3), 032002. https://doi.org/10.1088/1361-6501/ABC867

Lopatin, J., Kattenborn, T., Galleguillos, M., Perez-Quezada, J. F., & Schmidtlein, S. (2019). *Using aboveground vegetation attributes as proxies for mapping peatland belowground carbon stocks*. https://doi.org/10.1016/j.rse.2019.111217

Lu, B., & Hardin, J. (2021). A Unified Framework for Random Forest Prediction Error Estimation. In *Journal of Machine Learning Research* (Vol. 22). http://jmlr.org/papers/v22/18-558.html.

Markle, C. E., North, T. D., Harris, L. I., Moore, P. A., & Waddington, J. M. (2020). Spatial Heterogeneity of Surface Topography in Peatlands: Assessing Overwintering Habitat Availability for the Eastern Massasauga Rattlesnake. *Wetlands*, *40*(6), 2337–2349. https://doi.org/10.1007/S13157-020-01378-2/FIGURES/6

Mattivi, P., Franci, F., Lambertini, A., & Bitelli, G. (2019). TWI computation: a comparison of different open source GISs. *Open Geospatial Data, Software and Standards*, *4*(1), 1–12. https://doi.org/10.1186/s40965-019-0066-y

Maxwell, A. E., Warner, T. A., & Fang, F. (2018). Implementation of machine-learning classification in remote sensing: an applied review. *International Journal of Remote Sensing*, *39*(9), 2784–2817. https://doi.org/10.1080/01431161.2018.1433343

McFeeters, S. K. (1996). The use of the Normalized Difference Water Index (NDWI) in the delineation of open water features. *Https://Doi.Org/10.1080/01431169608948714*, *17*(7), 1425–1432. https://doi.org/10.1080/01431169608948714

Mickler, R. A., Welch, D. P., & Bailey, A. D. (2017). Carbon emissions during wildland fire on a North American temperate peatland. *Fire Ecology*, *13*(1), 34–57. https://doi.org/10.4996/fireecology.1301034

Minasny, B., Berglund, Ö., Connolly, J., Hedley, C., de Vries, F., Gimona, A., Kempen, B., Kidd, D., Lilja, H., Malone, B., McBratney, A., Roudier, P., O'Rourke, S., Rudiyanto, Padarian, J., Poggio, L., ten Caten, A., Thompson, D., Tuve, C., & Widyatmanti, W. (2019). Digital mapping of peatlands – A critical review. *Earth-Science Reviews*, *196*, 102870. https://doi.org/10.1016/j.earscirev.2019.05.014

Moore, P. A., Didemus, B. R., Furukawa, A., & Waddington, J. M. (2021). Peat depth as a control on Sphagnum moisture stress during seasonal drought. *Hydrological Processes*, *Press*. https://doi.org/10.1002/hyp.14117.

Moore, P. A., Lukenbach, M. C., Thompson, D. K., Kettridge, N., Granath, G., & Waddington, J. M. (2019). Assessing the peatland hummock-hollow classification framework using high-resolution elevation models: Implications for appropriate complexity ecosystem modeling. *Biogeosciences*, *16*(18), 3491–3506. https://doi.org/10.5194/BG-16-3491-2019

Nungesser, M. K. (2003). Modelling microtopography in boreal peatlands: hummocks and hollows. *Ecological Modelling*, *165*(2–3), 175–207. https://doi.org/10.1016/S0304-3800(03)00067-X

Ontario GeoHub. (2016). *Central Ontario Orthophotography (COOP) 2016*. https://geohub.lio.gov.on.ca/documents/lio::central-ontario-orthophotography-coop-2016/about

Poggio, L., Lassauce, A., & Gimona, A. (2019). Modelling the extent of northern peat soil and its uncertainty with Sentinel: Scotland as example of highly cloudy region. *Geoderma*, *346*, 63–74. https://doi.org/10.1016/j.geoderma.2019.03.017

Raduła, M. W., Szymura, T. H., & Szymura, M. (2018). Topographic wetness index explains soil moisture better than bioindication with Ellenberg's indicator values. *Ecological Indicators*, *85*, 172–179. https://doi.org/10.1016/j.ecolind.2017.10.011

Rampi, L. P., Knight, J. F., & Lenhart, C. F. (2014). Comparison of flow direction algorithms in the application of the cti for mapping wetlands in minnesota. *Wetlands*, *34*(3), 513–525. https://doi.org/10.1007/s13157-014-0517-2

Roger, E., & Ramp, D. (2009). Incorporating habitat use in models of fauna fatalities on roads. *Diversity and Distributions*, *15*(2), 222–231. https://doi.org/10.1111/J.1472-4642.2008.00523.X

Silva, C. A., Hudak, A. T., Vierling, L. A., Valbuena, R., Cardil, A., Mohan, M., Alves De Almeida, D. R., Broadbent, E. N., Zambrano, A. M. A., Wilkinson, B., Sharma, A., Drake, J. B., Medley, P. B., Vogel, J. G., Atticciati Prata, G., Atkins, J. W., Hamamura, C., Johnson, D. J., & Klauberg, C. (2022). treetop: A Shiny-based application and R package for extracting forest information from LiDAR data for ecologists and conservationists. *Methods in Ecology and Evolution*, *00*, 1–13. https://doi.org/10.1111/2041-210X.13830

Sørensen, R., Zinko, U., & Seibert, J. (2006). On the calculation of the topographic wetness index: evaluation of different methods based on field observations. *European Geosciences Union*, *10*(1), 101–112. https://hal.archives-ouvertes.fr/hal-00304825

Strobl, C., Boulesteix, A. L., Kneib, T., Augustin, T., & Zeileis, A. (2008). Conditional variable importance for random forests. *BMC Bioinformatics*, *9*(1), 1–11. https://doi.org/10.1186/1471-2105-9-307/FIGURES/4

Tang, J., Pilesjö, P., & Persson, A. (2013). Estimating slope from raster data – a test of eight algorithms at different resolutions in flat and steep terrain. *Geodesy and Cartography*, *39*(2), 41–52. https://doi.org/10.3846/20296991.2013.806702

Tashakor, S., Chamani, A., & Moshtaghie, M. (2023). Noise pollution prediction and seasonal comparison in urban parks using a coupled GIS- artificial neural network model. *Environmental Monitoring and Assessment*, *195*(2), 1–11. https://doi.org/10.1007/S10661-022-10858-3/TABLES/4

Tekatch, A. M., Wilkinson, S. L., Markle, C. E., & Waddington, J. M. (2023). Bottom-Up Controls on Fire Refugia in a Boreal Shield Landscape. *In press*.

Waddington, J. M., Morris, P. J., Kettridge, N., Granath, G., Thompson, D. K., & Moore, P. A. (2015). Hydrological feedbacks in northern peatlands. *Ecohydrology*, *8*(1), 113–127. https://doi.org/10.1002/eco.1493

Wilkinson, S. L., Tekatch, A. M., Markle, C. E., Moore, P. A., & Waddington, J. M. (2020). Shallow peat is most vulnerable to high peat burn severity during wildfire. *Environmental Research Letters*, *15*(10), 104032. https://doi.org/10.1088/1748-9326/aba7e8

Chapter 3: Examining the Relationship between Bulk Density and Peat Thickness

Background

Smouldering peatland fires are a significant concern due to the release of stored legacy soil carbon (Wilkinson et al., 2023), impacts on human health (Liu et al., 2015) and wildlife habitat (e.g. Markle et al., 2020). With the increase in peat fires due to climate change driven drying and other human impacts such as drainage (Turetsky et al., 2014) understanding what areas are potentially vulnerable to fire is key to being able to manage an ever-increasingly fire-prone landscape (Wilkinson et al, 2021).

Soil bulk density is one of many factors that impact peat vulnerability to smouldering (Benscoter et al., 2011; Wilkinson et al., 2019). Bulk density is calculated as the dry weight of soil divided by the in-situ volume. Peat with higher (organic soil) bulk density has more organic fuel per unit volume, which means there is more energy from smouldering to drive off soil moisture and heat the fuel to the ignition temperature, thereby increasing the likelihood that peat smouldering can propagate laterally and or vertically (Benscoter et al., 2011). This chapter provides two tools for better understanding peat bulk density in the context of peat fires and beyond.

Peat thickness, depth, and bulk density

Primarily, this chapter examines the relationship between peat thickness and bulk density. Here, peat thickness refers to the depth of the peat profile, from the surface

of the *Sphagnum* to the mineral soil or bedrock below. The term thickness is used rather than depth to avoid confusion with peat sample depth, defined as the distance below the surface where a peat sample was measured.

The relationship between peat sample depth and bulk density has been examined in a range of hydrogeological settings and hydrogeoclimatic regions (e.g. Clymo, 2004; Howard et al., 1995; Lewis et al., 2011; Novak et al., 2008; Tomlinson and Davidson, 2000; Weiss et al., 2002). Peat bulk density generally increases with depth, especially in the top 50 cm of the peat profile, although very deep peatlands (multiple meters) tend to show no change in bulk density with depth below that upper 50 cm until at least 500 cm (Clymo, 2004; Howard et al., 1995; Lewis et al., 2011; Tomlinson and Davidson, 2000; Wellock et al., 2011). This did not apply to peatlands with significant human impacts, which had bulk density – depth trends which were more closely linked to site-specific changes such as changes in agricultural practices (Novak et al., 2008). Nevertheless, the upper 50 cm of a relatively undisturbed *Sphagnum*-dominated peatland generally shows the trend of increasing bulk density with depth, because the top few centimeters of the peat profile is generally loose, live *Sphagnum*, or very weakly decomposed peat with a very high porosity. Larger fibrous plant matter particles in less decomposed peat generally correlates to low density peats (Nichols and Boelter, 1984) because the smaller plant debris fragments in more decomposed peat have a smaller proportion of large pore spaces (Rezanezhad et al., 2016). Further down in the profile, the

peat is denser due to the combined effects of peat consolidation during dry periods and many hundreds more years of decomposition (Rezanezhad et al., 2016).

While many studies have examined bulk density changes in peat profiles, a yet unresolved question is how the peat thickness impacts the rate of change in bulk density within a profile. The hypothesis investigated here is that deeper peats have a more gradual increase in bulk density with depth.

This is of particular importance in the context of wildfires for several reasons. The rate of change in bulk density is important as higher bulk densities (especially near the surface) are more likely to extend the smouldering of a fire (assuming low moisture conditions). All else being equal, if denser peats are nearer to the top of the profile where ignition occurs, deeper burning is more likely (Benscoter et al., 2011). This problem is magnified based on the interactions between moisture content and bulk density in a fire context. For example, Kohlenberg et al. (2018) found that depth of burn was related to the combined interactions of bulk density and moisture content. Specifically, they found that peat with higher bulk density was more vulnerable to deeper burning except for when the peat had high moisture content. As such, if bulk density is lower, then peat needs to be drier to continue burning than it would with a higher bulk density. Given that shallower peatlands have both denser peats nearer to the surface and are more likely to lose their water table in droughts (Moore et al., 2021), these shallow areas are especially at risk of deep burning. This furthers the explanation behind the “survival of the deepest” hypothesis proposed by Wilkinson et al. (2020) which suggests that deeper profiles

are less vulnerable to high-severity wildfire, because of the interaction between depth and the rate of increase in bulk density and moisture content. In addition, bulk density is important not just in terms of fire propagation/severity; as higher bulk density is related to higher carbon emissions in wildfires (Smith et al., 2018; Wijedasa, 2016). Peat with higher bulk densities nearer the surface of a peatland (in these shallow areas) would release carbon into the atmosphere for the same volume of peat burned.

Von Post and bulk density

Measuring bulk density directly requires taking field samples, transporting them to a lab, and doing multiple days of lab work. It is therefore difficult to measure rapidly and cost-effectively in the field (Al-Shammary et al., 2018; Chimner et al., 2014). As such, to increase the number of data points comparing bulk densities at different peat thicknesses (especially for use in future spatial modelling of bulk density) and to test a field approach that could be used by practitioners and wildfire managers, a method correlating a field variable with bulk density was tested. Subsetting to only sample bulk density at certain depths, an approach used by Chimner et al. (2014), was considered however sampling only certain depths would have required assumptions about the pattern in bulk density between those depths. Soil penetration resistance using a dynamic cone penetrometer (Herrick and Jones, 2002) at each point and correlating those measurements with a smaller subset of bulk density sampling was attempted but deemed infeasible due to large shrub roots stopping the penetrometer. Instead, Von Post (VP) measurements were

used. The Von Post humification scale was created for the Soil Survey of Sweden in 1926 to correlate peat properties with degree of composition of the peat (Andriesse, 1988; Von Post, 1922). It is a scale with ten points based on characteristics of the peat where one is a living layer of moss and 10 is a homogeneous organic material. This is measured subjectively through examining the peat and squeezing some peat in a hand and observing what is exuded from the hand. For example, peat with a VP of two is dead plant matter that is otherwise intact, and when squeezed, clear to yellowish water is emitted (Andriesse, 1988). Peat with a VP of six consists of about decomposed half plant matter, and dark brown water and a third of the peat escapes from the hand when squeezed (Andriesse, 1988). The VP method is quick, simple to learn, and can be implemented in the field, requiring no lab work. If a strong relationship exists between bulk density and VP, this method could be easily operationalized to help fire managers get a better understanding of the bulk density in peatlands and by extension a better understanding of potential smouldering vulnerability.

Relationships between VP and bulk density have been investigated in two other instances. In woody peats in northern Ontario, Silc and Stanek (1977) found a linear relationship increasing 0.02 g/cm^3 per each step up on the VP scale, ranging from 0.07 g/cm^3 to 0.23 g/cm^3 for the 10-point scale. A linear relationship was also found between VP and bulk density for *Sphagnum* peats in Finland, (Päivänen (1969), as cited in Verry et al., (2011)) (bulk density = 0.045 + 0.011VP, R^2 = 0.76). As such, applying this method is promising.

Study area

The primary study area, Dinner Lake, is situated around ~20 km north of Parry Sound, ON, Canada (45.457, -80.156) and is part of the Nibi (Water) Observatory for Boreal Ecohydrological Landscapes (NOBEL). The study area is within the Georgian Bay Biosphere Mnidoo Gamii, a UNESCO biosphere and is within the Robinson-Huron Treaty of 1850 and the Williams Treaty of 1923 and is located on Anishinabek territory. Additional data from another similar NOBEL site located on Henvey Inlet First Nation territory around ~10km north of Britt, ON, Canada (~45.860, -80.674) were collected as part of the same field campaign and used here to supplement the dataset. This latter site was adjacent to the location of the 2018 Parry Sound 33 (PS33) wildfire that burned over 11,000 ha.

The study area is a rock barrens and peatland landscape, part of the Boreal Shield ecozone (Markle et al., 2020; Moore et al., 2019). The area includes many peatlands and ephemeral wetlands of various sizes situated in depressions in the granite bedrock.

Methods

Field

Grids of nine points spaced with 3 m separation were randomly generated across the study area. At all peat grid points, VP measurements were taken manually at 5 cm intervals down the mineral layer or to 40 cm in depth, whichever was deeper. This maximum depth was chosen because measured depths of burn in the nearby PS33 fire never exceeded 40 cm (Wilkinson et al., 2020) and therefore peat

properties below that level are not as relevant for burning. Nevertheless, an additional 10 cm of depth was sampled (if possible) to provide further context. VP measurements were all taken by one individual for consistency. Intermediate VP measures (e.g., 4.5) were applied only if characteristics of multiple VP levels were present. At all points, peat thickness was measured using a probe inserted into the ground until solid resistance indicative of bedrock and/or a “gritty” texture indicating mineral soil was reached.

At one point per grid, amounting to approximately 10% of the total points, peat samples were taken for lab analysis. The central point was chosen except in cases where taking a core at that location was not feasible due to extremely dense roots, being deeply submerged, or other reasons. In these cases, samples were taken from another arbitrary point in the grid. This allowed for wide spatial distribution of sampling for the VP-bulk density relationship with representative sampling.

Samples were taken in 5 cm intervals from the top 45 cm of the peat profile using a box corer. Some peat profiles are less than 45 cm due to the peat depth at that location being under 45 cm, or difficulties with coring deeper due to impenetrable roots. Samples were approximately 5 cm x 5 cm x 5 cm in volume. Precise dimensions of samples were measured in field for volume measurements needed for lab bulk density calculation. Samples were kept cold in the field and frozen immediately upon daily return to the accommodations. They were kept frozen until analysis.

Overall, there are 310 points within these grid systems with VP data for the top 50 cm. Cores were taken at a subset of 43 of those points. Between those 43 profiles, a total of 287 peat samples, each representing a 5 cm subset of the profile, were separated and analyzed for bulk density and loss on ignition (LOI).

Lab

Samples were thawed and then oven-dried at 65° for 72 hours and weighed in the lab following drying to calculate weight for dry bulk density. Dried samples were also analyzed for LOI in a muffle furnace at 550°C for four hours to determine the proportions or mineral and organic content in the samples (Chambers et al., 2010).

Results and discussion

Bulk density and sample depth

Bulk density was positively related to depth in the top 45 cm for all profiles (n = 43, significant for eight profiles at $P < .001$, 17 profiles at $P < .01$, and eight profiles at $P < .05$) (Figure 3.1). The rate of increase is highly variable between profiles, and some profiles appear to have an inflexion point (e.g., 88E, 31C). Plots are ordered by peat thickness; the following section explains why there is variability in the relationship between bulk density and depth, examining several factors, most notably peat thickness.

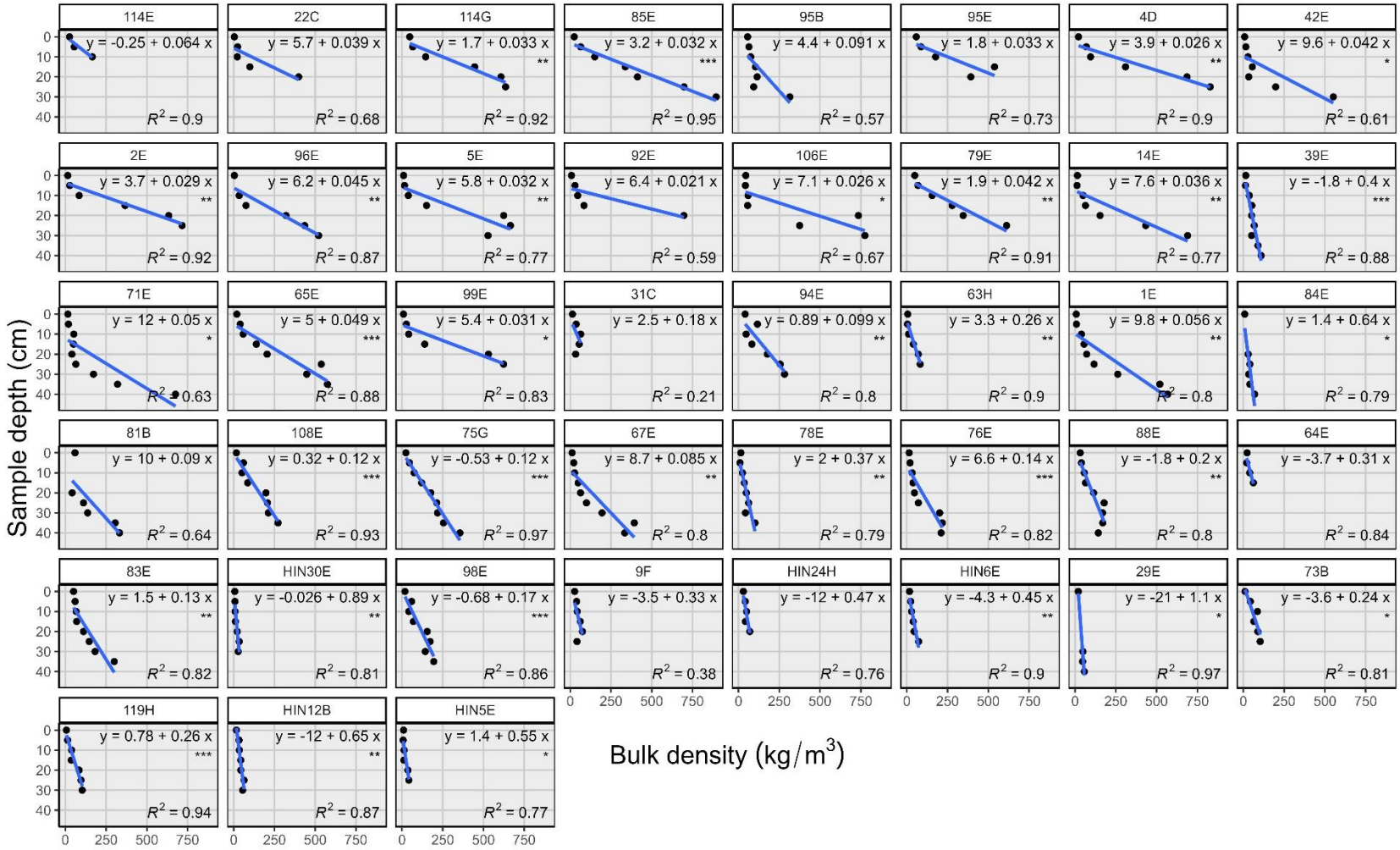

*Figure 3.1: Bulk density in 5 cm interval peat depths in the top 45 cm of peat in individual profiles. Best fit line shows linear relationship. Plots are ordered by peat thickness; 114E is the shallowest, HIN5E is the deepest). Asterisks show significance vales: ***P < .001, **P < .01, *P < .05.*

Bulk density and peat thickness

In Figure 3.2, the individual peat profiles are sorted by profile peat thickness. The grey bars represent the peat thickness. Each point on a corresponding bar represents a peat sample (a point plotted at 0 cm depth is sample from 0-5 cm). Colours indicate bulk density. Higher bulk densities are clustered lower down in peat profiles and at shallower peat thicknesses. It appears that peat samples taken closer to the bottom of a profile have higher bulk densities.

The depth of the sample and peat thickness appear to have interactive effects with bulk density. To examine the trend where points closer to the bottom of a profile seem to have higher bulk densities, the percentage of peat thickness that a sample was taken at was calculated. Lower numbers represent samples closer to the surface (for this analysis, the average depth of a sample was used to avoid 0 % depths, e.g., 2.5 cm was used for samples from 0 – 5 cm). High numbers represent peat samples closer to the bedrock or mineral soil underlaying the peatland.

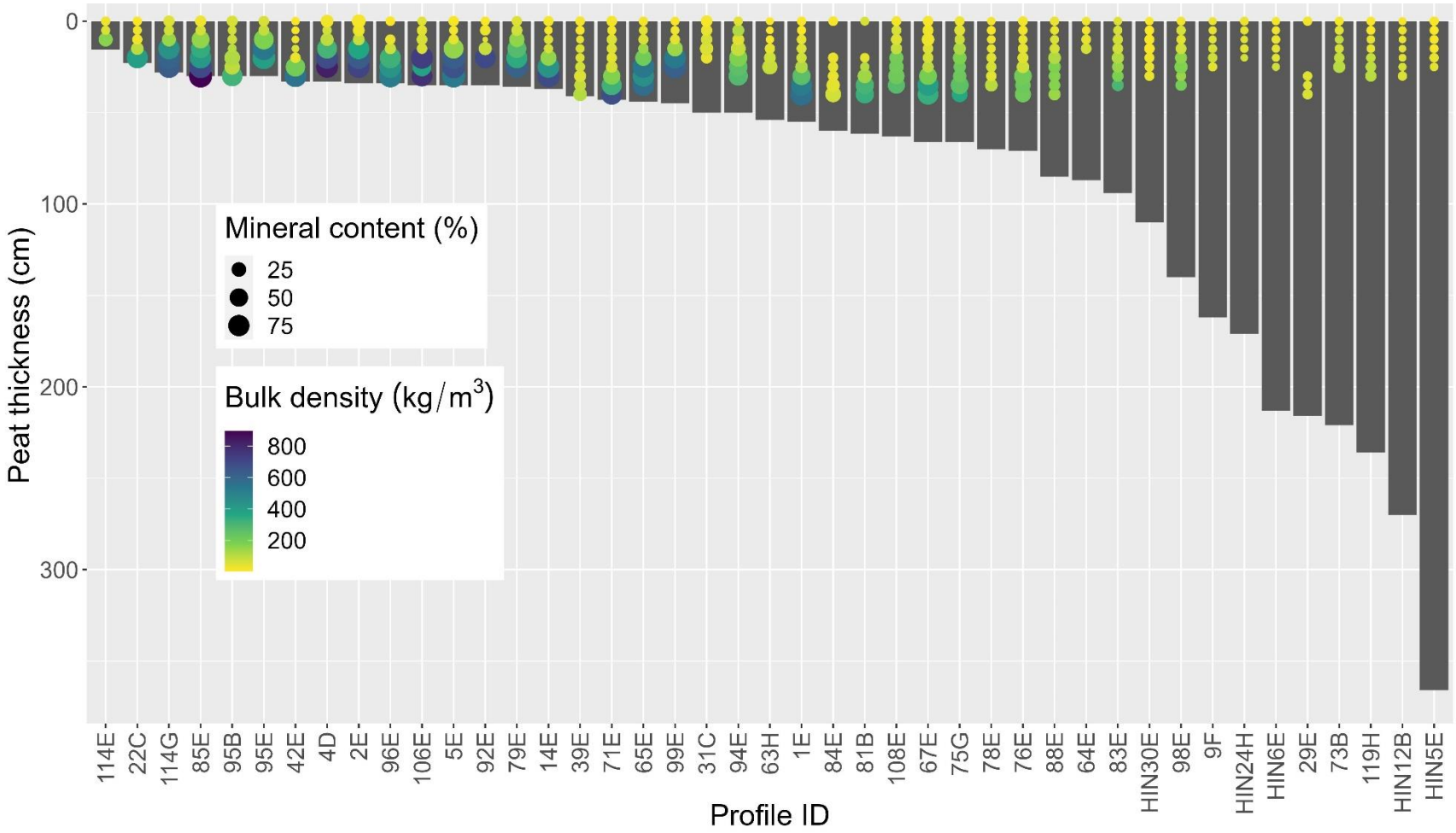

Figure 3.2: Overview of peat sample properties plotted at sample depth. This plot shows peat thickness (grey bars) of each profile, sorted from shallowest (left) to deepest (right). Each point is a peat sample. Point colour shows bulk density, and point size shows percent mineral by weight.

Figure 3.3 shows three variables (peat thickness, sample depth, and sample depth as a percentage of peat thickness) compared to bulk density. There appears to be a relationship between peat thickness and bulk density, however peat thickness alone does not explain very much of the variability in bulk density. R^2 values for linear models with any transformations were poor (maximum R^2 value of 0.11). There was a stronger relationship between sample depth and peat thickness (middle panel, R^2 of 0.47 with log of bulk density), however the strongest relationship was between the percentage of peat thickness variable (right panel, R^2 of 0.60 with log of bulk density). From this, we can infer that bulk density is not just increasing with sample depth but with the combined effects of sample depth and overall peat thickness.

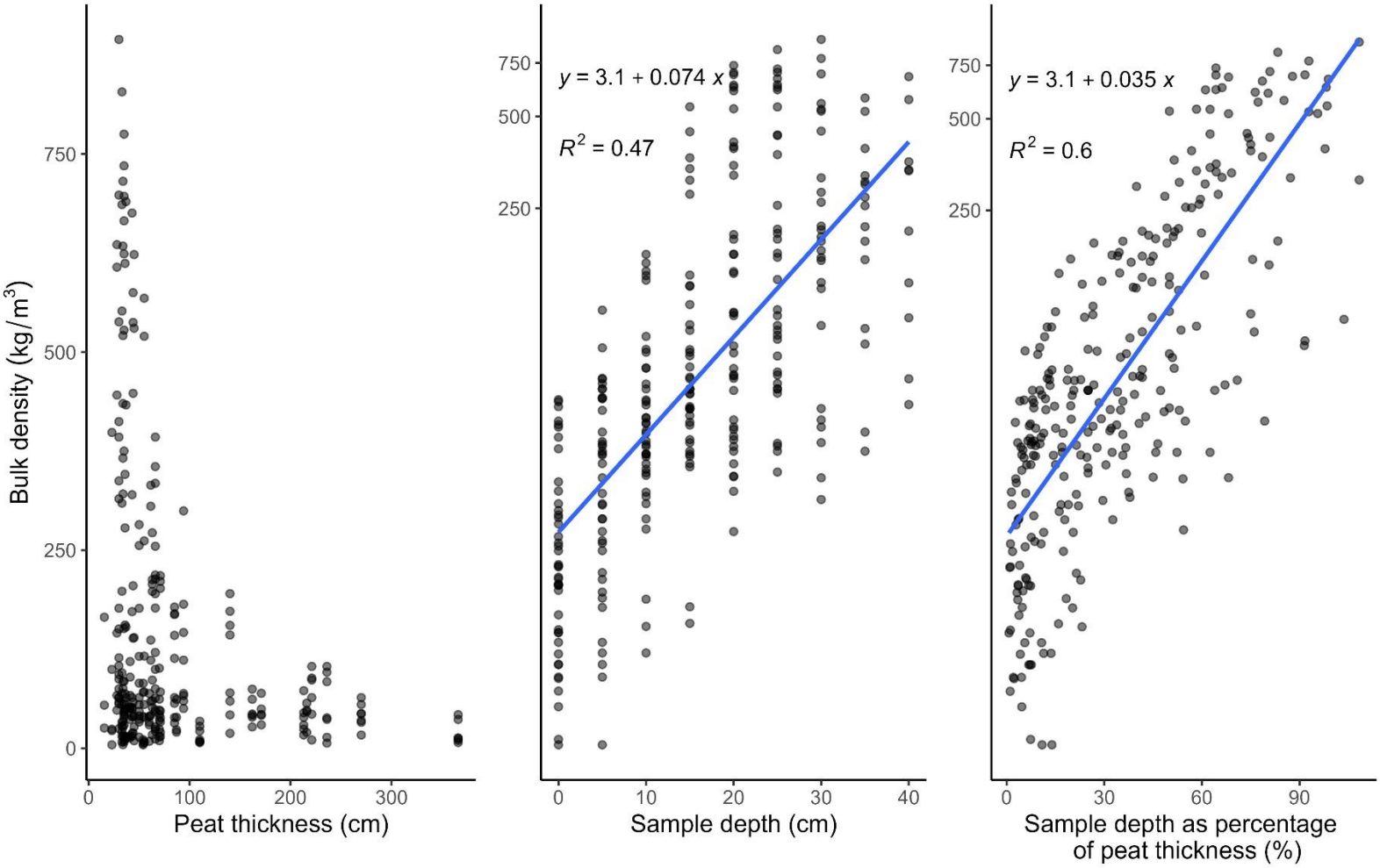

Figure 3.3: Peat thickness and depth variables and bulk density. From left to right, panels show peat thickness, sample depth, and sample depth as a percentage of profile thickness. Y axes for the second and third panels are shown with log-transformation for better linear model fit; y in the displayed equations is log(bulk density).

Mineral content and decomposition controls on bulk density

To further investigate why bulk density is controlled by both peat thickness and sample depth, additional variables were examined in their relationships with bulk density, peat thickness, and sample depth. Figure 3.4 examines these relationships.

Mineral content, defined here as the percentage of soil weight remaining after ignition in a furnace at 550° for four hours, is compared to bulk density on the left plot in Figure 3.4. The linear relationship is highly correlated (R^2 = 0.86). This is expected due to the higher specific gravities of inorganic particles compared to organic particles (Huat et al., 2009; Li et al., 2020). Figure 3.4 also reveals that samples with high mineral content tend to be from profiles with lower peat thickness (shown as smaller-sized points). This may be because lower peat thicknesses mean samples are relatively closer to the bedrock or mineral soil layer below, meaning that mineral soil processes have a greater possibility of influencing the peat (Parry and Charman, 2013). All the samples at the surface of the peat profile (shown as yellow/light-coloured points) are very low in both bulk density and mineral content. In addition, the low-mineral content samples have a clear trend where samples closer to the peat surface have lower bulk densities: mineral content is not the only variable controlling bulk density. This suggests that factors like compression and decomposition of the organic portion of the peat are also important.

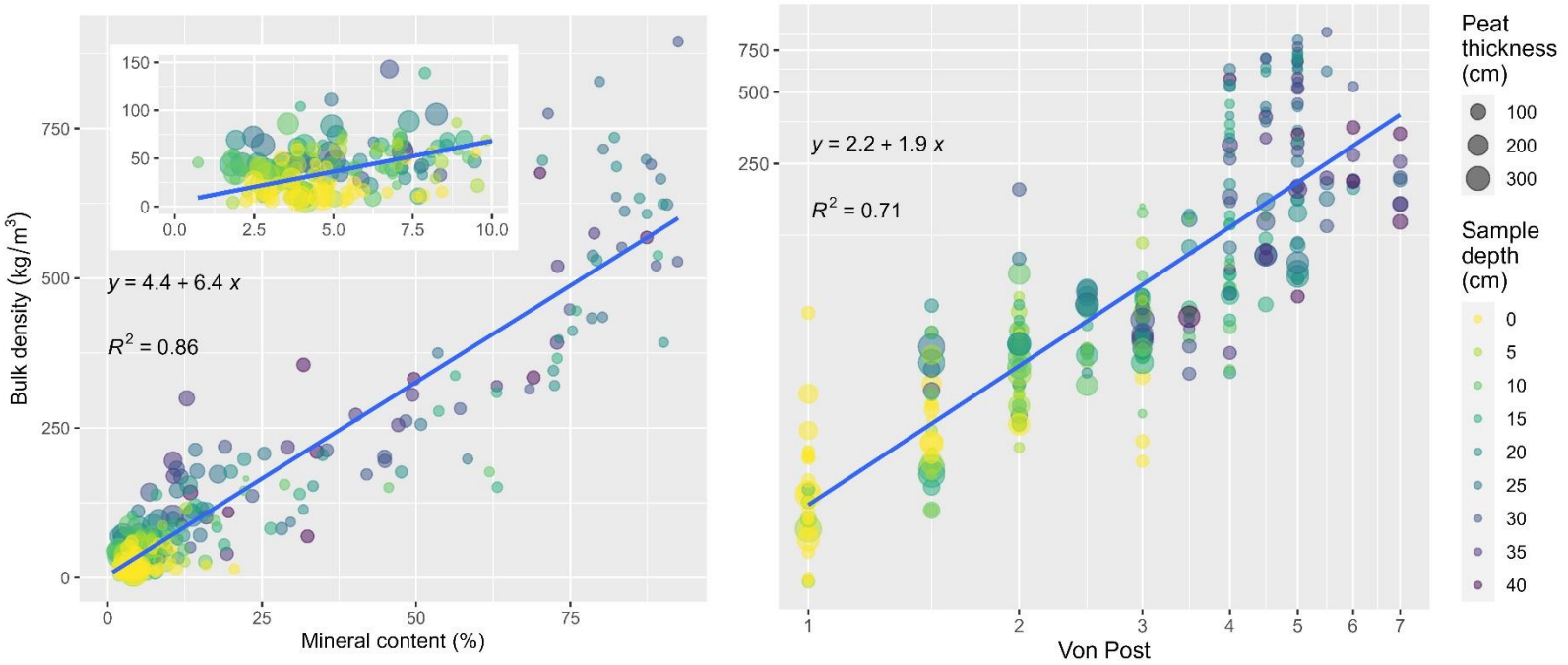

Figure 3.4: Other sample properties and bulk density. The left plot shows mineral content. The inset plot shows an enlarged view of the same plot, showing only the section with mineral contents less than 10%. The right plot shows bulk density and VP. Note natural log scale on both axes. For this equation, y and x refer to log(bulk density) and log(VP), respectively. On both plots, colours show sample depth and point size shows peat thickness.

The plot on the right in Figure 3.4 shows the relationship between VP (from field data) and bulk density, where higher bulk densities generally have higher VPs: higher levels of decomposition. A log – log relationship was found to have the best fit ($R^2 = 0.71$). This differs from previously-found VP and bulk density relationships, where an untransformed linear model was used by both Silc and Stanek (1977) and Päivänen (1969, as cited in Verry et al. (2011)).The non-linear relationship found here may exist due to the confounding effects of increased decomposition on other soil properties which in turn impact bulk density. For example, less decomposed soils have higher compressibility (Rezanezhad et al., 2016) which would relate to greater bulk density. Nonetheless, the strong fit suggests that VP could be used as a proxy for bulk density in some cases where lab measurements are not operationally feasible given resource constraints, as discussed in the background section. VP also show a clear positive relation with to sample depth: as expected, there is increasing decomposed peat with depth (peat at depth is older and has been decomposing for a longer period of time).

Using the larger dataset of all points with VP (n = 2539) (Figure 3.5), it appears that for peat profiles with thicknesses less than 100 cm, VP increases more quickly with depth in shallow profiles; however, for points greater than 100 cm, there appears to be minimal effect of peat thickness and VP increases with sample depth at a similar rate across these profiles. At sample depths of 35, 40, and 45 cm, there are notable peaks in VP around peat thicknesses of 150 cm, however these are

likely due to data distribution issues, as there is a lack of data around those depths and thicknesses due to factors such as impassible tree roots preventing sampling.

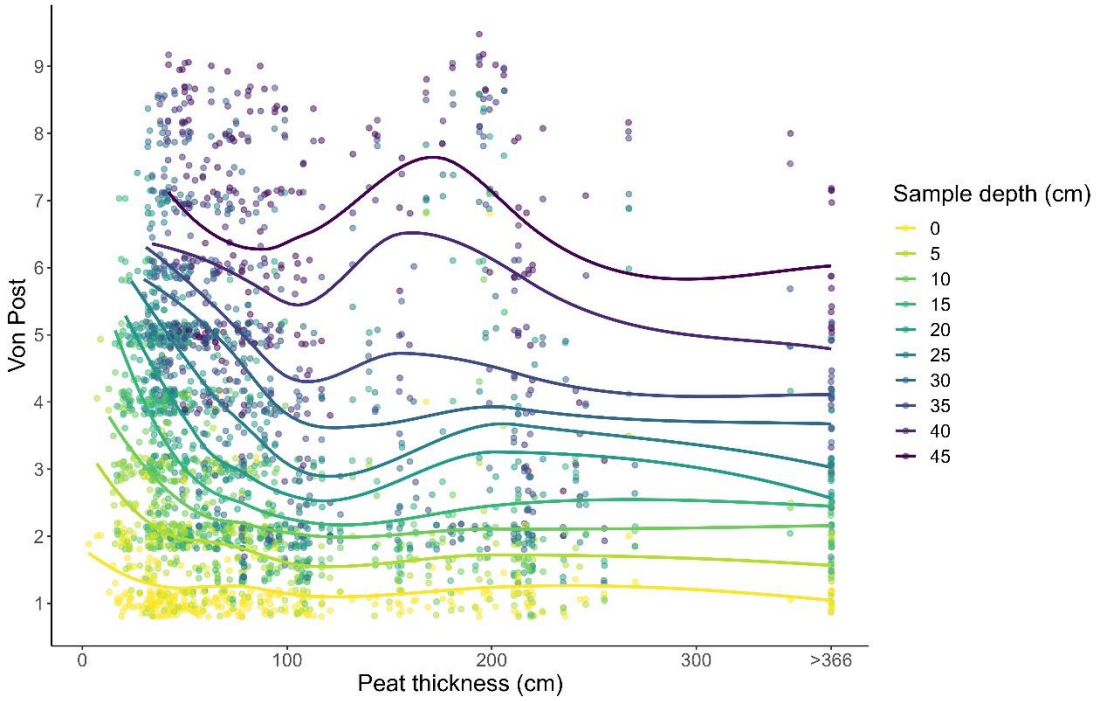

Figure 3.5: Peat thickness and VP for a larger number of peat profiles. Jitter is applied to point for improved visualization as VP is categorical. Colour shows sample depth. Lines were generated with Loess smoothing. Lines for higher sample depths have fewer data points and have considerably higher standard error (not shown here for improved clarity of plot). Many peat profiles were deeper than probe depth (366 cm) and so are plotted at > 366 cm, therefore the lines may not represent the true relationship at that range.

The two different trends between VP and peat thickness, divided at a peat thickness of approximately 100 cm may be because similar decomposition processes (e.g., anaerobic and aerobic chemical and microbial decomposition processes) are happening throughout all profiles vertically, but in the shallower peats, these processes are condensed into a limited vertical space.

Linear mixed effects model

A linear mixed effects model was used to statistically verify these findings. The model considers each individual sample bulk density as the sampling unit (dependent variable). The model aims to determine if is there still an impact of peat thickness (the “fixed effect”), when peat sample depth (the “random effect”) is controlled for. Based on study design, peat profile ID was also included as a random effect. This model result was significant at $P < .001$, with either fixed or random slopes set (random slopes allows for different bulk density-thickness relationships at different sample depths). This confirms that thicker peats have lower bulk densities at the same depths.

Notably, if you also control for mineral content in 10% categories and VP (as random effects), the fixed slope model becomes not significant and the random slope model is only significant at $P < .05$. As such, it could be concluded that the relationship between peat thickness and bulk density is predominantly attributable to the effects of the mineral content and decomposition as they both vary with depth. It is especially related to mineral content: 88% of the total variance was attributed to the mineral content in the fixed slope model.

Organic bulk density and mineral bulk density

Given the control mineral content has on the thickness-bulk density relationship, weighted organic bulk density (OBD, calculated as bulk density x organic fraction from LOI, and representing the mass of organic matter per volume of soil) and weighted mineral bulk density (MBD, calculated as bulk density x mineral fraction

and representing the mass of mineral particles per volume of soil) were examined. Figure 3.6 shows MBD and OBD relationships with peat thickness. The different components of bulk density have different types of interactions with depth and thickness: high MBDs are only found in shallow peatlands, at deeper sample depths. When these high mineral bulk densities are present, they control bulk density as MBDs are much greater than the OBDs. These especially high MBDs are found only in samples with increasingly high sample depth with peat thickness: they are found only at very high percentages of profile depths (Figure 3.7).

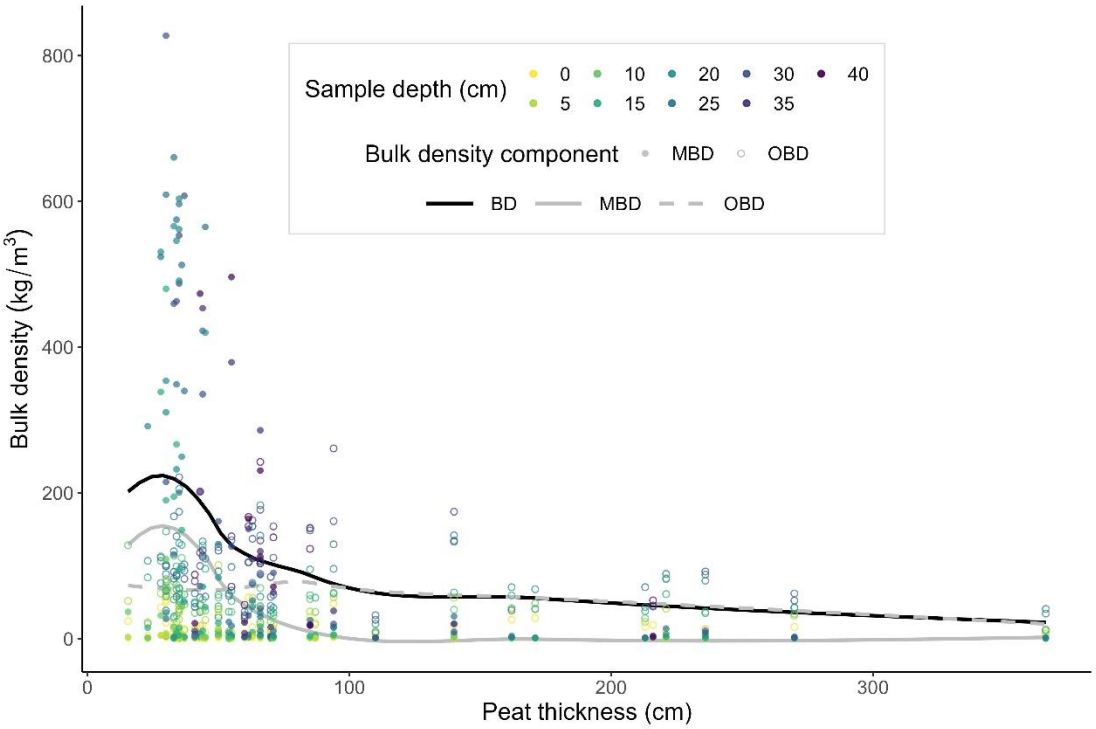

Figure 3.6: OBD and MBD compared to peat thickness and sample depth. MBD is shown by solid grey line and dots; OBD is shown by circles and dashed grey line. Trendlines were generated with Loess smoothing. Note that standard error is high for the trendlines in peat thicknesses greater than ~ 100 cm due to relatively small number of samples.

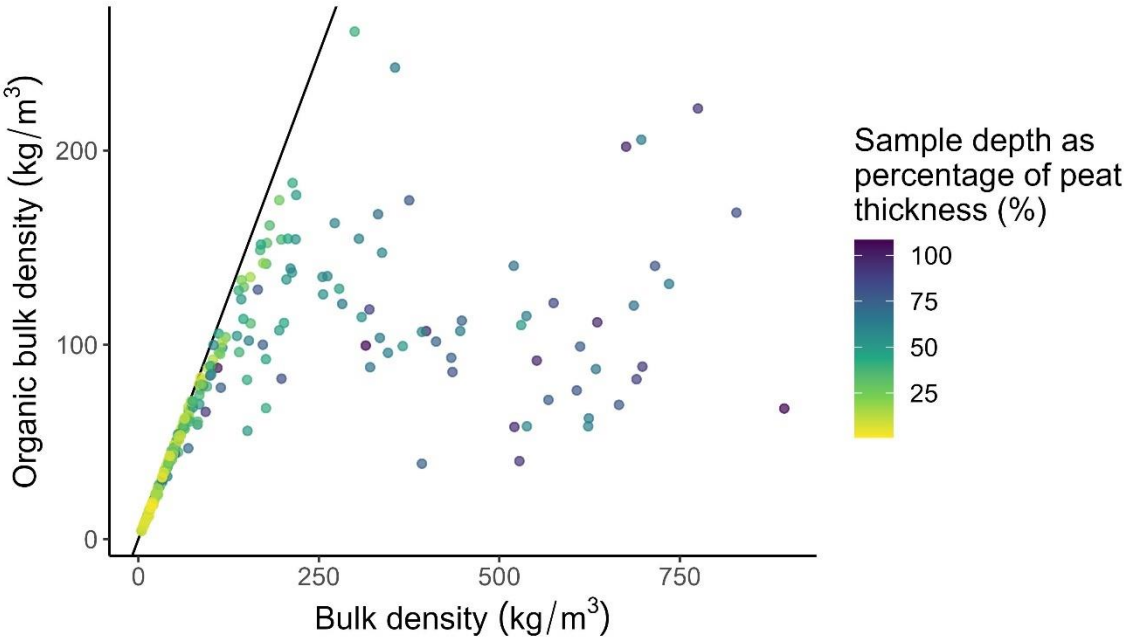

Figure 3.7: OBD and bulk density, colored by percentage of peat thickness. Black line shows where OBD is equal to bulk density, which is the case if MBD is negligible. Samples further from the black line have higher MBDs.

However, for peatlands where the total thickness is greater than approximately 100 cm, bulk density in the upper 45 cm of peat is controlled by OBD, since OBDs are much greater than MBDs, which are consistently low. While this appears to have a decreasing trend with peat thickness in Figure 3.6, this may be due to the relatively small sample size at higher thicknesses: standard error is considerable. OBDs do continue to increase with peat sample depth, as expected. This is consistent with the relationship between VP and peat thicknesses and depths in the thicker profiles. That being said, considering OBDs across all depths, another trend visible in Figure 3.6 is that OBDs are still lower in thicker peat profiles, which again matches the trends found in the more data-rich VP dataset (Figure 3.5). The change in measured OBDs with sample depths is much greater in the shallower

peat profiles therefore while MBD is more important in overall OBD, the organic matter is still also higher in these shallow peat profiles as would be expected based on VP. In the upper 10 cm of peat depth, even in the shallow sites, MBD is still low (Figure 3.8). OBD controls bulk density at the top of the profiles, and shallow sites have higher OBDs than deeper sites.

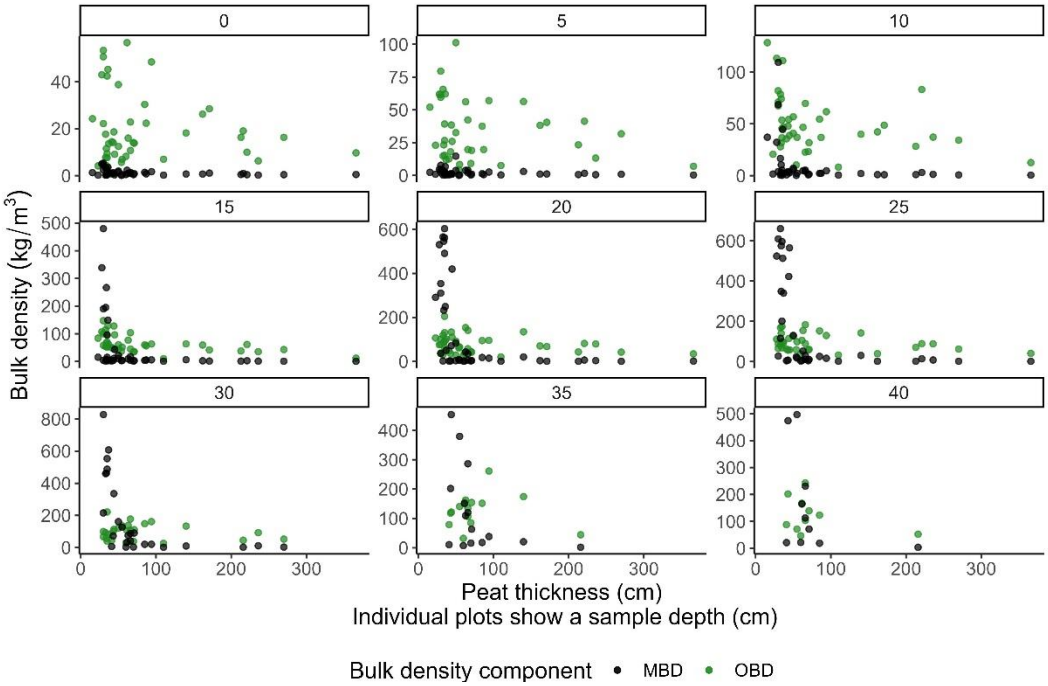

Figure 3.8: OBD and MBD by peat thickness, shown at individual sample depths for comparison. Note different y axis scales on plot; this allows for more detailed comparison.

Hydrological controls on bulk density

An additional factor that may be controlling the overall bulk density – peat thickness relationship in addition to mineral content and peat decomposition is peat compression. Deeper peatlands are less susceptible to drying during drought periods (Moore et al., 2021), therefore, assuming most shallow peats are in

shallower peatlands, they are more likely to have experienced drying cycles in the past and at the time of sampling. As peat readily expands with wetting (Morton and Heinemeyer, 2019; Rezanezhad et al., 2016), higher moisture conditions in the peat when the peat was sampled (as would be expected in thicker peatlands in dry conditions) would relate to higher volumes and therefore lower bulk densities, though this relationship has been shown to by hysteretic (Price and Schlotzhauer, 1999). Moisture data was taken during sampling only in the top 5 cm of the profile of all points sampled (including VP points); there did not appear to be a trend with profile depth, or a trend between moisture and bulk density for the small number of surface points this data was available for (n = 37).

Furthermore, deeper peats would also potentially have higher bulk densities due to other feedbacks across long time periods. With optimal water availability, moss production is higher, so moisture retention in peat leads to *Sphagnum* growth (Waddington et al., 2015). This again would lead to lower bulk densities in thicker peatlands. Also, lower water table position means there would be more oxygen availability, which contributes to increased decomposition (Waddington et al., 2015). Microbial activity has been found to the highest in depths of peat with fluctuating water table (Lin et al., 2014), so potentially higher water table fluctuations associated with shallower peat would also lead to higher levels of decomposition.

Data regarding peat profile depths in relation to average peatland depth or water table depth data within a peatland were not explicitly collected as part of this study,

however given the availability of the peat depth map generated in Chapter 2, and large number of long-term water table datasets in the NOBEL study areas, there is opportunity for further study.

Conclusion

In the top 45 cm of peat, higher bulk densities are found further from the surface of peatlands in thicker peat profiles. However, this relationship was primarily controlled by the high mineral contents of peat close to the bottom of shallow peat profiles. This has important and complex implications for peatland smouldering vulnerability. Higher mineral content in the shallow sites may protect them from deeper smouldering, as the mineral soil components absorb the energy produced by the fire. This contrasts the often-held view that higher bulk density peat soils are more vulnerable to fire due to their higher fuel contents. Gravimetric moisture content of peat, which is the ratio of volumetric water content to bulk density, has been suggested as a measure of peat vulnerability to smouldering given that gravimetric moisture content would represent the ratio of energy sink to available fuel (Benscoter et al., 2011). This would *not* be applicable in this context, given the high mineral content in shallow peat which contrasts the negligible mineral content in the Alberta boreal bogs studied by Benscoter et al. (2011). Not only does bulk density not correspond to increased fuel in some of the presently studied peat samples, but it would also likely correspond to an energy sink in the high-mineral content soils found at low peat thicknesses. Conversely, mineral content does also enhance heat transfer because of its higher heat conductivity (Huang and Rein,

2015). Overall, however, added mineral content in peat decreases the level of moisture that a soil is capable of burning with (Frandsen, 1987). Considering porosity and other hydrologic processes, high bulk density has been shown to be positively related to volumetric water retention (Moore et al., 2014) again possibly correlating these shallow-profile peats with lower vulnerability to fire. More relevantly, in peat-mineral mixes, volumetric water holding capacity was found to increase, but gravimetric water holding capacity decreased, with increasing organic soil content due to the confounding effects of bulk density (Moskal et al., 2011). Specific yield, or the level to which a water deficit would decrease the water table is another property linked with the relationship between peat smouldering and bulk density by Wilkinson et al. (2019), but was not investigated here; but because higher bulk density peat often has smaller pore sizes and therefore lower specific yield, the high bulk density shallow peats found here still may be more vulnerable to drying out and therefore more vulnerable to fire. Furthermore, shallower peats still had higher OBDs, and higher decomposition based on VP at equivalent sample depths compared to deeper profiles, so there is still relatively more fuel, which is important in terms of both burn severity and carbon release in fire.

While dense peats with bulk densities greater than the 100 kg/m^3 noted by Luckenbach et. al (2015) to be part of the conditions allowing for severe smouldering to propagate deep in the profile were found, it is unlikely that these peats would act in the same way, given that many (but not all) peat samples with

bulk densities > 100 kg/m^3 measured had high bulk densities because of their elevated mineral contents.

Finally, mineral content impacts on bulk density are predominantly below the top 15 cm of peat. While this means that as fire burns downwards in the peat profile it will eventually hit a layer with too much mineral soil to continue smouldering (Rein, 2013), it also means that given the still relatively high organic bulk densities of peats in the top of the shallower profiles, the top parts of these profiles will still (as previous research suggests) be more vulnerable to smouldering and liable to release more carbon when burnt, compared to the thicker peats.

Overall, peat bulk density was found to increase more quickly with depth in shallower peat thicknesses. However, because the increase with depth was primarily attributable to changes in mineral content in depths closer to the bottom of the peat profile in some shallow samples, the high bulk densities of these would not drastically increase vulnerability to fire. In addition, the bulk density – peat thickness – depth relationship is still evident when considering only organic bulk densities. This is attributable to decomposition processes and hydrological processes happening differently at different peat thicknesses. Therefore, there is still higher fuel content, and likely lower moisture retention abilities (due to their higher bulk densities) closer to the surface in shallow peatlands, making them likely more vulnerable to fire.

Literature cited

Al-Shammary, A. A. G., Kouzani, A. Z., Kaynak, A., Khoo, S. Y., Norton, M., & Gates, W. (2018). Soil Bulk Density Estimation Methods: A Review. *Pedosphere*, *28*(4), 581–596. https://doi.org/10.1016/S1002-0160(18)60034-7

Andriesse, J. P. (1988). *Nature and management of tropical peat soils*. Food and Agriculture Organization of the United Nations.

Benscoter, B. W., Thompson, D. K., Waddington, J. M., Flannigan, M. D., Wotton, B. M., de Groot, W. J., & Turetsky, M. R. (2011). Interactive effects of vegetation, soil moisture and bulk density on depth of burning of thick organic soils. *International Journal of Wildland Fire*, *20*(3), 418–429. https://doi.org/10.1071/WF08183

Chambers, F. M., Beilman, D. W., & Yu, Z. (2010). Methods for determining peat humification and for quantifying peat bulk density, organic matter and carbon content for palaeostudies of climate and peatland carbon dynamics. *Mires and Peat*, *7*.

Chimner, R. A., Ott, C. A., Perry, C. H., & Kolka, R. K. (2014). Developing and Evaluating Rapid Field Methods to Estimate Peat Carbon. *Wetlands*, *34*, 1241–1246. https://doi.org/10.1007/s13157-014-0574-6

Clymo, R. S. (2004). Hydraulic conductivity of peat at Ellergower Moss, Scotland. *Process*, *18*, 261–274. https://doi.org/10.1002/hyp.1374

Frandsen, W. H. (1987). The influence of moisture and mineral soil on the combustion limits of smoldering forest duff. *Canadian Journal of Forest Research*, *17*(12), 1540–1544. https://doi.org/10.1139/x87-236

Herrick, J. E., & Jones, T. L. (2002). A dynamic cone penetrometer for measuring soil penetration resistance. *Soil Science Society of America Journal*, *66*(4), 1320–1324. https://doi.org/10.2136/sssaj2002.1320

Howard, P. J. A., Loveland, P. J., Bradley, R. I., Dry, F. T., Howard, D. M., & Howard, D. C. (1995). The carbon content of soil and its geographical distribution in Great Britain. *Soil Use and Management*, *11*(1), 9–15. https://doi.org/10.1111/J.1475-2743.1995.TB00488.X

Huang, X., & Rein, G. (2015). Computational study of critical moisture and depth of burn in peat fires. *International Journal of Wildland Fire*, *24*(6), 798. https://doi.org/10.1071/WF14178

Huat, B. B. K., Asadi, A., & Kazemian, S. (2009). Experimental Investigation on Geomechanical Properties of Tropical Organic Soils and Peat. *American Journal of Engineering and Applied Sciences*, *2*(1), 184–188.

https://doi.org/10.3844/AJEASSP.2009.184.188

Kohlenberg, A. J., Turetsky, M. R., Thompson, D. K., Branfireun, B. A., & Mitchell, C. P. J. (2018). Controls on boreal peat combustion and resulting emissions of carbon and mercury. *Environmental Research Letters*, *13*(3), 035005. https://doi.org/10.1088/1748-9326/aa9ea8

Lewis, C., Albertson, J., Xu, X., & Kiely, G. (2011). *Spatial variability of hydraulic conductivity and bulk density along a blanket peatland hillslope*. https://doi.org/10.1002/hyp.8252

Li, W., O'Kelly, B. C., Yang, M., Fang, K., Li, X., & Li, H. (2020). Briefing: Specific gravity of solids relationship with ignition loss for peaty soils. *Geotechnical Research*, *7*(3), 134–145. https://doi.org/10.1680/JGERE.20.00019/ASSET/IMAGES/SMALL/JGERE7-0134-F6.GIF

Lin, X., Tfaily, M. M., Green, S. J., Steinweg, J. M., Chanton, P., Imvittaya, A., Chanton, J. P., Cooper, W., Schadt, C., & Kostka, J. E. (2014). *Microbial Metabolic Potential for Carbon Degradation and Nutrient (Nitrogen and Phosphorus) Acquisition in an Ombrotrophic Peatland*. https://doi.org/10.1128/AEM.00206-14

Liu, J. C., Pereira, G., Uhl, S. A., Bravo, M. A., & Bell, M. L. (2015). A systematic review of the physical health impacts from non-occupational exposure to wildfire smoke. *Environmental Research*, *136*, 120–132. https://doi.org/10.1016/j.envres.2014.10.015

Markle, C. E., North, T. D., Harris, L. I., Moore, P. A., & Waddington, J. M. (2020). Spatial Heterogeneity of Surface Topography in Peatlands: Assessing Overwintering Habitat Availability for the Eastern Massasauga Rattlesnake. *Wetlands*, *40*(6), 2337–2349. https://doi.org/10.1007/S13157-020-01378-2/FIGURES/6

Markle, C. E., Wilkinson, S. L., & Waddington, J. M. (2020). Initial Effects of Wildfire on Freshwater Turtle Nesting Habitat. *The Journal of Wildlife Management*, *84*(7), 1373–1383. https://doi.org/10.1002/jwmg.21921

Moore, P. A., Morris, P. J., & Waddington, J. M. (2014). Multi-decadal water table manipulation alters peatland hydraulic structure and moisture retention. *Hydrological Processes*, *29*(13), 2970–2982. https://doi.org/10.1002/HYP.10416

Moore, Paul A., Didemus, B. R., Furukawa, A., & Waddington, J. M. (2021). Peat depth as a control on Sphagnum moisture stress during seasonal drought. *Hydrological Processes*, *Press*. https://doi.org/10.1002/hyp.14117.

Moore, Paul A., Lukenbach, M. C., Thompson, D. K., Kettridge, N., Granath, G.,

& Waddington, J. M. (2019). Assessing the peatland hummock-hollow classification framework using high-resolution elevation models: Implications for appropriate complexity ecosystem modeling. *Biogeosciences*, *16*(18), 3491–3506. https://doi.org/10.5194/BG-16-3491-2019

Morton, P. A., & Heinemeyer, A. (2019). Bog breathing: the extent of peat shrinkage and expansion on blanket bogs in relation to water table, heather management and dominant vegetation and its implications for carbon stock assessments. *Wetlands Ecology and Management*, *27*(4), 467–482. https://doi.org/10.1007/S11273-019-09672-5

Moskal, T. D., Leskiw, L., Naeth, M. A., & Chanasyk, D. S. (2011). Effect of organic carbon (peat) on moisture retention of peat:mineral mixes. *Https://Doi.Org/10.4141/S00-011*, *81*(2), 205–211. https://doi.org/10.4141/S00-011

Nichols, D. S., & Boelter, D. H. (1984). Fiber Size Distribution, Bulk Density, and Ash Content of Peats in Minnesota, Wisconsin, and Michigan. *Soil Science Society of America Journal*, *48*(6), 1320–1328. https://doi.org/10.2136/SSSAJ1984.03615995004800060024X

Novak, M., Brizova, E., Adamova, M., Erbanova, L., & Bottrell, S. H. (2008). Accumulation of organic carbon over the past 150 years in five freshwater peatlands in western and central Europe. *Science of The Total Environment*, *390*(2–3), 425–436. https://doi.org/10.1016/J.SCITOTENV.2007.10.011

Parry, L. E., & Charman, D. J. (2013). Modelling soil organic carbon distribution in blanket peatlands at a landscape scale. *Geoderma*, *211–212*(1), 75–84. https://doi.org/10.1016/j.geoderma.2013.07.006

Price, J., & Schlotzhauer, S. M. (1999). Importance of shrinkage and compression in determining water storage changes in peat: the case of a mined peatland. *Hydrological Processes*. https://doi.org/10.1002/(SICI)1099-1085(199911)13:16

Rein, G. (2013). Smouldering Fires and Natural Fuels. *Fire Phenomena and the Earth System: An Interdisciplinary Guide to Fire Science*, 15–33. https://doi.org/10.1002/9781118529539.CH2

Rezanezhad, F., Price, J. S., Quinton, W. L., Lennartz, B., Milojevic, T., & Cappellen, P. Van. (2016). *Structure of peat soils and implications for water storage, flow and solute transport: A review update for geochemists*. https://doi.org/10.1016/j.chemgeo.2016.03.010

Silc, T., & Stanek, W. (1977). Bulk Density Estimation of Several Peats in Northern Ontario using the Von Post Humification Scale. *Canadian Journal of Soil Science*, *57*, 75. https://cdnsciencepub.com/doi/pdf/10.4141/cjss77-010

Smith, T. E. L., Evers, S., Yule, C. M., & Gan, J. Y. (2018). In Situ Tropical Peatland Fire Emission Factors and Their Variability, as Determined by Field Measurements in Peninsula Malaysia. *Global Biogeochemical Cycles*, *32*(1), 18–31. https://doi.org/10.1002/2017GB005709

Tomlinson, R. W., & Davidson, L. (2000). Estimates of carbon stores in four northern Irish lowland raised bogs. *Suo*, *51*(3), 169–179.

Turetsky, M. R., Benscoter, B., Page, S., Rein, G., Van Der Werf, G. R., & Watts, A. (2014). Global vulnerability of peatlands to fire and carbon loss. *Nature Geoscience 2015 8:1*, *8*(1), 11–14. https://doi.org/10.1038/ngeo2325

Verry, E. S., Boelter, D. H., Päivänen, J., Nichols, D. S., Malterer, T., & Gafni, A. (2011). *Physical Properties of Organic Soils*.

Von Post, L. (1922). *Sveriges Geologiska Undersöknings torvinventering och några av dess hittills vunna resultat.* https://doi.org/10.3/JQUERY-UI.JS

Waddington, J. M., Morris, P. J., Kettridge, N., Granath, G., Thompson, D. K., & Moore, P. A. (2015). Hydrological feedbacks in northern peatlands. *Ecohydrology*, *8*(1), 113–127. https://doi.org/10.1002/eco.1493

Weiss, D., Shotyk, W., Rieley, J., Page, S., Gloor, M., Reese, S., & Martinez-Cortizas, A. (2002). *The geochemistry of major and selected trace elements in a forested peat bog, Kalimantan, SE Asia, and its implications for past atmospheric dust deposition*.

Wellock, M. L., Reidy, B., Laperle, C. M., Bolger, T., & Kiely, G. (2011). Soil organic carbon stocks of afforested peatlands in Ireland. *Forestry: An International Journal of Forest Research*, *84*(4), 441–451. https://doi.org/10.1093/FORESTRY/CPR046

Wijedasa, L. S. (2016). Peat soil bulk density important for estimation of peatland fire emissions. *Global Change Biology*, *22*(9), 2959–2959. https://doi.org/10.1111/GCB.13364

Wilkinson, S. L., Moore, P. A., & Waddington, J. M. (2019). Assessing Drivers of Cross-Scale Variability in Peat Smoldering Combustion Vulnerability in Forested Boreal Peatlands. *Frontiers in Forests and Global Change*, *2*, 84. https://doi.org/10.3389/ffgc.2019.00084

Wilkinson, S. L., Tekatch, A. M., Markle, C. E., Moore, P. A., & Waddington, J. M. (2020). Shallow peat is most vulnerable to high peat burn severity during wildfire. *Environmental Research Letters*, *15*(10), 104032. https://doi.org/10.1088/1748-9326/aba7e8

Chapter 4: Conclusion

Climate change and other human activities are increasing the extent, severity, and frequency of peat smouldering and the concomitant negative impacts on humans, ecosystems, and carbon (e.g., Wilkinson et al., 2023). As such, there is a need to develop a better understanding smouldering vulnerability on the landscape, and to develop tools to do so.

Peat that is low in moisture, high in organic bulk density, and low in mineral content is most vulnerable to severe (deep) burning (Benscoter et al., 2011; Wilkinson et al., 2019). These deep burning conditions, particularly the tendency to have low moisture in drought conditions, have been correlated with shallower peatlands (Wilkinson et al., 2020), and the shallower margins of peatlands Wilkinson et al., 2019). As such, peat depth mapping may be of particular use for both peatland and wildfire management. However, available methods for mapping peat depth either require very intensive fieldwork, use not readily available remotely sensed data, or is not be precise enough to show details at a landscape level (Minasny et al., 2019).

As such, this thesis piloted the mapping of peat depths in a heterogeneous Ontario landscape at a 1 m spatial resolution using only two more readily available remotely sensed data products: COOP orthophotography and LiDAR. Rather than trying to directly map peat depths, machine learning was used to predict peat depths based on relationships between ecohydrological variables which relate to peatland formation processes.

A forest-based regression model was used, and predictor variables relating to hydrology, topography, and vegetation were generated from the LiDAR and COOP data. These data were trained by the model on a dataset of 1383 peat depths from field data. The model had a final R^2 value of 0.73, though based on a relatively small test dataset, it also had an MAE of 28 cm, and tended to overpredict lower peat depths, limiting its utility from a wildfire perspective. Training and testing the model with a greater number of points is suggested to improve accuracy. Specifically, the model had the highest uncertainty in floating peat mats and then in the middles of deep peatlands; generally, uncertainty was higher in areas with deeper predicted peat depths. While these areas are less relevant from a smouldering perspective, increasing training data points collected from these landscape features may help improve the model (this was not possible due to COVID-19 fieldwork restrictions). The most important predictor variables used in the model were TPI (representing topographic position within the landscape), NDVI: SD (a measure of vegetation variability), distance to nearest tree, and LiDAR ground intensity (a measure of forest inundation), confirming that a combination of ecological, hydrological, and topographic processes control organic soil formation in this landscape. Based on the resulting model map, most of the peat that is shallow enough to be vulnerable to fire but deep enough to be an important carbon source during smouldering is found in relatively small landscape patches. This may be complicated for landscape management, and reinforces the need for precise peat depth mapping, to identify these vulnerable areas.

The second chapter of this thesis examined the bulk density of peatlands in the same study area, specifically exploring the relationship between bulk density and peat depth (referred to henceforth as peat thickness) in the top 45 cm of peat profiles. As expected, peat bulk density increased with sample depth within a profile. In addition, in thicker profiles, bulk density was found to increase more gradually with depths – in other words, at the same sample depth, bulk densities were found to be lower in thicker samples. This relationship was found to be primarily controlled by the relatively high mineral content measured for some peat samples in profiles with thicknesses less than ~ 100 cm and sample depths below the top 10 - 15 cm of soil. Considering only the mineral fraction of the soil, mineral bulk densities were increasingly high in samples found relatively closer to the bottom of the peat profile, suggesting an influence of the mineral soil or bedrock below. Nonetheless, the organic fraction of soil still had higher bulk densities closer to the top of profiles in shallower peats. Although samples taken in the top 100 cm of peat had lower bulk densities (and lower both mineral and organic components) than peats below this approximate cutoff, the trend of decreasing peat bulk densities with peat thickness did not appear to continue above thickness around ~ 100 cm. This was also true for decomposition (as measured by VP), which is likely the main factor controlling bulk density at higher depths, given the relatively low mineral contents. Nevertheless, VP still had a similar trend to bulk densities in the < 100 cm range, wherein samples taken from shallower profiles had higher VP

values nearer to the surface of the peatland. The overall log (bulk density) - log (VP) relationship found corresponded well (R^2 = 0.71), suggesting that VP may be used as a simpler proxy for bulk density when a rapid field method is needed.

Accordingly, there are important implications for smouldering vulnerability in this landscape. In shallower peats, the top of the profile is especially vulnerable given high bulk densities (which are related to increased potential for the peat to dry out in droughts given hydrological properties that have been shown in the literature to correlate with higher bulk density soil), and also higher organic bulk densities (therefore more fuel contributing to smouldering propagation) compared to the near-surface peat in thicker peat areas. However, many of these shallow peatlands have higher mineral content in soil approaching the bottom of the peatland; the mineral-organic mix of these soils may prevent the smouldering from continuing towards the bottom of these profiles.

Overall, in this landscape, shallow peats are found in small pockets (as shown in the peat depth map) and may be more vulnerable to smouldering based on their higher bulk densities closer to the peat surface, in addition to their increased potential for low moisture levels in dry periods. Tools presented here such as the proposed method for peat depth mapping, and the use of VP as a proxy for bulk density, may be useful tools for peatland, wildfire, and land managers to identify areas highly vulnerable to smouldering.

Literature cited

Benscoter, B. W., Thompson, D. K., Waddington, J. M., Flannigan, M. D., Wotton, B. M., de Groot, W. J., & Turetsky, M. R. (2011). Interactive effects of vegetation, soil moisture and bulk density on depth of burning of thick organic soils. *International Journal of Wildland Fire*, *20*(3), 418–429. https://doi.org/10.1071/WF08183

Minasny, B., Berglund, Ö., Connolly, J., Hedley, C., de Vries, F., Gimona, A., Kempen, B., Kidd, D., Lilja, H., Malone, B., McBratney, A., Roudier, P., O'Rourke, S., Rudiyanto, Padarian, J., Poggio, L., ten Caten, A., Thompson, D., Tuve, C., & Widyatmanti, W. (2019). Digital mapping of peatlands – A critical review. *Earth-Science Reviews*, *196*, 102870. https://doi.org/10.1016/j.earscirev.2019.05.014

Wilkinson, S. L., Andersen, R., Moore, P. A., Davidson, S. J., Granath, G., & Waddington, J. M. (2023). Wildfire and degradation accelerate northern peatland carbon release. *Nature Climate Change 2023 13:5*, *13*(5), 456–461. https://doi.org/10.1038/s41558-023-01657-w

Wilkinson, S. L., Tekatch, A. M., Markle, C. E., Moore, P. A., & Waddington, J. M. (2020). Shallow peat is most vulnerable to high peat burn severity during wildfire. *Environmental Research Letters*, *15*(10), 104032. https://doi.org/10.1088/1748-9326/aba7e8

Wilkinson, S. L., Moore, P. A., & Waddington, J. M. (2019). Assessing Drivers of Cross-Scale Variability in Peat Smoldering Combustion Vulnerability in Forested Boreal Peatlands. *Frontiers in Forests and Global Change*, *2*, 84. https://doi.org/10.3389/ffgc.2019.00084